

# WIRELESS ENGINEER

Vol. 32

JULY 1955

No. 7

## Compression and Expansion of Programme Time

**I**N broadcasting, it sometimes happens that the length of an item does not precisely fit the time allocated to it in a programme. A speech, for example, may run naturally for 17 minutes, but there may be only 15 minutes available for it, or it may be required to accommodate the length of run of background music to the main item. It is then desired to compress an item in time, or sometimes expand it.

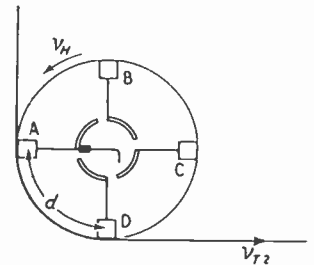
With recording, there are several possible ways of doing this, apart from the obvious one of editing the tape or disk to delete unimportant material. The medium can be run at a different speed in reproducing than the one used for recording, but there is the serious objection to this of an inevitable change of pitch.

Magnetic recording might provide another method, with interesting possibilities, by which the signal is compressed in time by having, as it were, small segments punched out of it at regular intervals and the resulting gaps closed up. In principle, one might cut the tape into a large number of bits all the same length, snip a small piece off each, and then join them together. The complete tape would obviously be shorter and, when run at its normal speed, would occupy less time. When an expansion, instead of a compression, in time is wanted, the bits of tape could be joined by new bits repeating the adjacent information, so that the whole tape is lengthened.

Similar effects to these can be obtained without actually cutting the tape by using a special reproducing system. One of the first, if not the first, applications of this idea was to the reproduction of recorded telegraph signals, so that they could be slowed up without alteration

of pitch. The German Tonschreiber B<sup>1</sup> operated on this principle. More recently, it has been applied to speech<sup>2</sup> and the method employed is quite ingenious. In the reproducer, the magnetic tape runs past a series of reproducing heads which are carried by a rotating drum and connected in turn to the output by a commutator.

The arrangement is sketched in the figure in which a drum is shown carrying four heads A-D. The sampling is carried out by these rotating heads which are switched into circuit by the commutator for the interval that



the particular head is in contact with the tape.

Head A is in contact with the tape from 9 o'clock to 6 o'clock, during which period the commutator selects the output of head A. Head B then comes into the 9 o'clock position and in contact with the tape and the commutator then disconnects A and connects B, and so on.

Providing the relative speed of the tape past the heads is the same as the recording speed, then the reproduced pitch is the same as the recorded pitch, but if the heads are moving in the direction shown, the actual speed of the tape can be greater than the recorded speed and the time of playing the tape is reduced. Thus if the original recording tape speed is  $v_{T_1}$  the reproducing tape speed is  $v_{T_2}$  and the proportion of playing time saved compared with the original playing time is  $(v_{T_2} - v_{T_1})/v_{T_2}$ .

If the relative velocity past the heads is to be maintained at  $v_{T_1}$  then  $v_{T_2} - v_H = v_{T_1}$  where  $v_H$  is the peripheral speed of the head, and the proportional time saved is  $v_H/v_{T_2}$  or  $v_H/(v_{T_1} + v_H)$ . When  $v_H$  is zero no time is saved; when  $v_H$  is equal to  $v_{T_2}$  there is 100% compression.

Consideration of the figure will show how this sampling process is achieved. The time taken for a head to move through  $d$  is  $d/v_H$  and in this time the tape moves  $v_{T_2} \times d/v_H$ . After this period the commutator switch will take the output of head B and thus length  $d$  of the tape will be unscanned. Thus in a total tape length of  $d(1 + v_{T_2}/v_H)$  a length  $d$  of tape remains unscanned. The time interval of information lost is  $d/v_{T_1}$  and is independent of the speeds  $v_{T_2}$  and  $v_H$  involved in reproduction.

In attempting to judge the suitability of this method for programme compression, two important criteria impose a limiting value on the period  $d/v_{T_1}$ . First, all essential characteristics contributing to fidelity must be retained, and secondly, the change in signal value during that period must be sufficiently small to avoid a rhythmic discontinuity which would give rise to flutter. Although work has been done to determine the minimum sampling time necessary to preserve intelligibility, so far as we are aware little is known about the effect on fidelity.

Gabor<sup>3</sup> states that if there is simultaneous pick up from heads located at a distance corresponding to 25 milliseconds difference of time, then the observer is not disturbed, but his ear adapts itself to an echo condition. In the present case, the heads are switched progressively and, without detailed tests, it is not possible to give a maximum delay defining the boundary between acceptable and unacceptable coloration. The change in magnitude of a programme signal during the unscanned period might easily amount to 1 db per 10 milliseconds, and the reproduced reverberation characteristic will be in a series of steps. This stepped signal is similar to that produced by the reverberation machine described by Axon, Gilford and Shorter<sup>4</sup> although with this no gap occurs between the steps. These discontinuities are rhythmic and if sufficient they give rise to flutter, but for lesser values a coloration in the signal may occur. In assessing the importance of these effects it must be remembered that a distance between the reproducing heads  $d$  equal to 1 in. corresponds to a time period of 67 milliseconds if the recording were made at 15 in. per second. It would seem that this interval is too long and a much closer spacing of heads is desirable. If the tape were recorded specially for compression a higher recording speed could be used but, if the method is to be applied to ordinary records, then standard speeds must be assumed. Although

no definite limits can be laid down, the evidence indicates that the time gap should be limited to about 10-15 milliseconds, which would limit the head spacing to under  $\frac{1}{4}$  in. The frequency of this discontinuity is given by  $v_H/d$  and for small amounts of compression  $v_H$  is low. For example, for 5% compression on a normal tape recorded at 15 in. per second,  $v_H$  is less than 1 in. per second and, if it were possible to locate the heads on the reproducer  $\frac{1}{4}$  in. apart, the discontinuity would occur four times a second. Schiesscr in his article mentions an element length of 2 cm corresponding to 26.6 milliseconds recording interval for a recording speed of 75 cm/sec. He says that the distortion is not noticeable under these conditions.

As the compression ratio increases  $v_H$  increases and less and less of the tape is scanned, and more elements of information that are required to maintain fidelity are lost.

The same relative speed could be achieved if  $v_H - v_{T_2} = v_{T_1}$  but, as the relative velocity between tape and head is now reversed, the tape would be scanned backwards. Although at first sight this condition appears worthless, under some circumstances it might be of interest. Referring again to the figure, it is evident that if  $v_H$  is greater than  $v_{T_2}$ , then while a head is moving from A to B the tape will move  $d \times v_{T_2}/v_H$ , and the length of tape scanned will be  $d - dv_{T_2}/v_H$  and the length unscanned  $dv_{T_2}/v_H$ . If the degree of compression is small then  $v_{T_2} \approx v_{T_1}$  and  $v_H \approx 2v_{T_2}$ , and the length of the unscanned tape is about  $d/2$ , but the length of scanned tape is also only about  $d/2$ . The periodicity of the discontinuities is still given by  $v_H/d$ , but for 5% compression  $v_H$  is now about 31 in. per sec instead of 1 in. per sec and for  $\frac{1}{4}$ -in. spacing the periodicity of the discontinuities is about 124 per second instead of four per second. If  $d$  could be made sufficiently small, and therefore the time length of the sample sufficiently small, the much higher periodicity of the discontinuities might prove an advantage.

The case of compression has been considered but expansion is equally possible and to be desired. Referring back to the figure, the heads must rotate in a direction opposite to the tape and the tape speed slowed down for expansion. Using the same symbols, if the pitch is to remain constant  $v_{T_2} - v_H = v_{T_1}$ . The proportional increase of playing time is  $(v_{T_1} - v_{T_2})/v_{T_2}$  which is equal, as before, to  $v_H/v_{T_2}$ . As before, the mechanism of the expansion can be seen by considering the relative motion of the heads and tape. The time taken for head to move through  $d$  is  $d/v_H$  and the tape moves during this period  $v_{T_2} \times d/v_H$ . In this case the movements are in opposite directions and therefore in a tape length

$d(1 + v_{T_2}/v_H)$  a length of tape  $d$  is scanned twice. As before, the time interval of information duplicated is independent of the reproduction speeds  $v_{T_2}$  and  $v_H$  and is equal to  $d/v_{T_1}$ . In this case there is no loss of information but the conditions regarding discontinuities still persist, and the repetition rate of the discontinuities remains at  $v_H/d$ .

The success of this method for the purpose discussed depends, as might be expected, on the sampling rate, which in turn, depends on the spacing of the heads that can be arranged conveniently on a drum. Further work will have to be done to determine the limiting value of spacing, but it appears to represent a severe mechanical

problem. The ability to increase or shorten the length of a programme by up to 10% would be of considerable value, if it could be done without editing, change of pitch or the introduction of unwanted coloration.

A. R. A. R.

### REFERENCES

<sup>1</sup> "The Magnetophon Sound Recording and Reproducing System", by M. J. L. Pulling, B.I.O.S. Final Report No. 951 (H.M. Stationery Office).  
<sup>2</sup> "Method for Time or Frequency Compression and Expansion of Speech", by Grant Fairbanks, W. L. Everitt and R. P. Jaeger, I.R.E. National Convention Paper, 26th March 1953, *Trans. Inst. Radio Engineers*, January-February 1954.  
<sup>3</sup> "A Device for Time Expansion used in Sound Recording", by H. Schiesser, *Funk und Ton*, 1949, Vol. 3, No. 5.  
<sup>4</sup> "New Possibilities in Speech Transmission", by D. Gabor, *J. Instn. elect. Engrs*, Part III, Nov. 1947, Vol. 94, No. 32.  
<sup>5</sup> "Artificial Reverberation", by P. E. Axon, C. L. S. Gilford and D. E. L. Shorter (Recent Paper read at I.E.E.).

# OPTIMUM SHAPE COILS

*For Producing Magnetic Fields*

By L. Lewin

(Standard Telecommunication Laboratories, Enfield, Middlesex)

## 1. Introduction

THE problem has arisen of providing a magnetic field at the centre of a given cylinder with a minimum expenditure of power. The solution to this problem does not appear to be available in the literature and it seemed worth while to record the present analysis which led to an appropriate formula.

## 2. General Formula

Fig. 1 shows a coil wound on a cylinder of radius  $a$  (cm). At radius  $y$  the length of the coil is  $2af(y/a)$  where  $f$  is a function which determines the shape of the coil. The coil is wound with wire of radius  $r$  and resistivity  $\rho$  (ohm-cm). It is assumed that the wires are wound in contact within a layer, and with layers exactly above each other, to give a packing factor  $\pi r^2/4r^2 = 0.79$ . Then the magnetic field  $H$  at the centre of the coil axis is

$$H = \frac{\pi I a}{10r^2} \int_1^{Y_0} \frac{f(Y) dY}{[Y^2 + f^2(Y)]^{3/2}} \text{ oersteds} \quad (1)$$

Here  $I$  (amps) is the current in the coil, and  $Y = y/a$  is a dimensionless variable of integration.  $Y_0$  is the value of  $Y$  at the greatest radius.

The power  $P$  (watts) supplied to the coil is  $P = I^2 R$  where the resistance  $R$  is given by

$$R = \frac{\rho a^3}{r^4} \int_1^{Y_0} Y f(Y) dY \text{ ohms.} \quad (2)$$

Eliminating  $I$  and  $r$  from equation (1) gives

MS accepted by the Editor, July 1954

$$H = \frac{\pi}{10} \sqrt{\frac{P}{\rho a}} F \quad (3)$$

where

$$F = \int_1^{Y_0} \frac{f(Y) dY}{[Y^2 + f^2(Y)]^{3/2}} / \left[ \int_1^{Y_0} Y f(Y) dY \right]^{\dagger}$$

$F$  is a form factor, and depends only on the shape of the coil, as determined by  $f(Y)$ . Apart from the variation due to  $F$ , equation (3) shows that  $H$  is proportional to the square root of the available power, and inversely to the root of the inner coil radius.

## 3. Optimum coil

In the appendix it is shown that  $F$  has a maximum value of 0.512 when the function  $f$  has the form

$$f(Y) = [4.905 Y^{2/3} - Y^2]^{\dagger} \quad (4)$$

$Y_0$ , the maximum value of  $Y$ , is 3.292.

The shape of this optimum coil is shown in Fig. 1.

## 4. Rectangular Coil

In general, a rectangular shaped coil is to be preferred to that given by equation (4). What

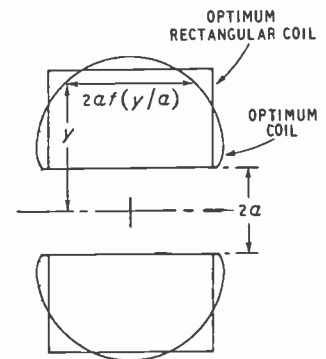


Fig. 1. Optimum coils.

is the best shape, and how much does  $F$  drop below its maximum value?

When  $f(Y)$  is constant the integration in (3) gives

$$F = \left[ \frac{2f}{Y_0^2 - 1} \right]^{\frac{1}{2}} \log_e \frac{Y_0 + (Y_0^2 + f^2)^{\frac{1}{2}}}{1 + (1 + f^2)^{\frac{1}{2}}} \quad (5)$$

This function has a maximum value of 0.505 when  $Y_0 = 3.10$  and  $f = 1.86$ . This optimum rectangular coil is also shown in Fig. 1. The magnetic field is only 1% below its maximum as given by (4).

### 5. Sub-Optimal Rectangular Coils

It may happen that further requirements are put on the desired magnetic field, such as an extension of the region in which it should maintain its value. In this case it may be necessary to depart from the optimum size; and equation (5) shows how the field will drop.

Fig. 2. shows the form factor  $F$  plotted against the length/internal diameter ratio,  $f$ , for a series of values of the external/internal diameter ratio,  $Y_0$ . The fall from the optimum value can be easily seen from these curves.

The use of a sub-optimal coil is sometimes a convenient way of meeting, in part, the impedance requirements of a given power supply.

for the optimum  $f(Y)$  depend only on  $Y_0$ . Putting the first equal to  $\frac{1}{2} \alpha^{3/2}$  times the second (this form is chosen for convenience only) it is found that

$$\int \left\{ \alpha^{3/2} [Z^2 + f^2(Z)]^{3/2} - Z \right\} \delta f(Z) dZ = 0.$$

Since  $\delta f(Z)$  is arbitrary we must have the remaining factor in the integrand zero, whence

$$f(Z) = [\alpha Z^{2/3} - Z^2]^{\frac{1}{2}}.$$

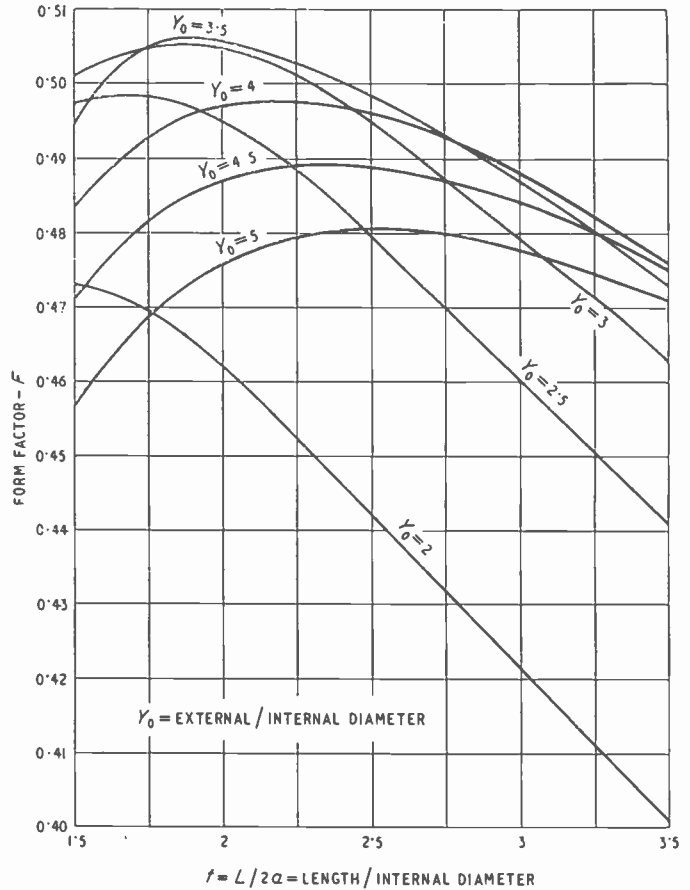


Fig. 2. Sub-optimal rectangular coils.

### APPENDIX

Put  $A = \int \frac{f dY}{(Y^2 + f^2)^{\frac{1}{2}}}$ ,  $B = \int Y f dY$

Then  $F^2 = A^2/B$ , and  $\delta F^2 = 2AB^{-1} \delta A - A^2 B^{-2} \delta B$ . Hence  $F$  is optimal when  $\delta F = 0$ , or  $2B \delta A = A \delta B$ . Introducing a double integral notation, so that products of integrals are expressed as double integrals, it is found that

$$\iint \left\{ Y f(Y) \left[ \frac{2 \delta f(Z)}{[Z^2 + f^2(Z)]^{\frac{3}{2}}} - \frac{2 f^2(Z) \delta f(Z)}{[Z^2 + f^2(Z)]^{5/2}} \right] - \frac{f(Y)}{[Y^2 + f^2(Y)]^{\frac{1}{2}}} Z \delta f(Z) \right\} dY dZ = 0$$

Carrying out the  $Y$  integrations involves  $\int_1^{Y_0} Y f(Y) dY$  and  $\int_1^{Y_0} \frac{f(Y) dY}{[Y^2 + f^2(Y)]^{\frac{1}{2}}}$ . The values of these two integrals,

It remains to determine  $\alpha$ , which is given, from its definition, by

$$\int_1^{Y_0} Y [\alpha Y^{2/3} - Y^2]^{\frac{1}{2}} dY = \frac{1}{2} \alpha \int_1^{Y_0} Y^{1/3} [2 Y^{2/3} - Y^2]^{\frac{1}{2}} dY$$

$Y_0$  is given by the greatest value of  $Y$  for which the length of the coil is a real quantity; i.e., by  $\alpha Y_0^{2/3} - Y_0^2 = 0$ , or  $Y_0 = \alpha^{3/4}$ . The integrals can be evaluated in terms of elliptic functions. Putting  $\alpha = \sec^4 \phi$  the equation becomes, after some reduction

$$\cos^3 \phi \left( \frac{13 - 10 \cos^4 \phi}{3} \right) \left[ \frac{1 - \cos^4 \phi}{2} \right]^{\frac{1}{2}} = 2E(\phi) - F(\phi) \quad (6)$$

mod  $k = \sin 45^\circ$

In terms of  $\phi$ , the form factor is

$$F = 2 \cos^3 \phi (1 - \cos^4 \phi)^{3/4}$$

Equation (6) has the solution  $\phi = 47.8^\circ$ , whence  $F = 0.512$ , and the optimum coil shape is

$$f(Y) = [4.905 Y^{2/3} - Y^2]^{\frac{1}{2}}.$$

# TRANSIENT RESPONSE CALCULATION

## Approximate Method for Minimum Phase-Shift Networks

By Dharmajit Gupta Sarma, M.Sc.

(Institute of Radio Physics & Electronics, Calcutta University)

**SUMMARY.**—The well-known method of linear segments for the calculation of zero-pole locations of the transfer function corresponding to a given attenuation characteristic is extended by allowing the zeros and the poles to assume complex instead of only real values. The extension removes some of the limitations of the method and thus enlarges its range of applicability; at the same time it yields results which are more accurate. The extended method has been applied for calculating the transient response of minimum phase-shift type networks from the attenuation versus frequency characteristic.

### 1. Introduction

THE transient response of a system may, in principle, be calculated from the Fourier Integral equation

$$f(t) = \frac{1}{\pi} \int_0^{\infty} A_0(\omega) \cos[\omega t - \phi(\omega)] d\omega \quad (1)$$

where  $f(t)$  is the response of the system to Dirac's  $\delta$  function input,

$A_0(\omega)$  is the steady-state attenuation characteristic of the system as a function of frequency,

$\phi(\omega)$  is the steady-state phase shift characteristic of the system as a function of frequency.

This direct method of calculating the transient response is generally lengthy and cumbersome. It is, however, not so for the large class of networks known as minimum phase-shift networks. This is because in such networks the attenuation and phase-shift characteristics are not independent of one another; if one is known, the other is deducible from it. Generally the attenuation characteristic is given and the phase-shift characteristic is calculated therefrom to obtain the transient response. Even this calculation can be avoided and the transient response obtained directly, if the zero and pole locations of the transfer function of the system are found from the attenuation characteristic. Approximate methods have been developed for such calculations of the zero-pole locations, and are usually resorted to in the design of attenuation equalizers. Of these various methods the semi-graphical method of linear segments is probably the simplest in application.

The object of the linear segment method is to find an arrangement of zeros and poles of a transfer function which represents approximately the given attenuation characteristic. This is done by approximating the given characteristic by a number of straight-line segments in a suitable manner,

as explained in the next section. The method, however, suffers from certain limitations regarding the choice of the lengths of the segments as also their slopes with reference to the frequency axis. In the present paper an extension of the method is discussed. The extension enlarges to a great extent the scope of applicability of the method by removing the limitations and, at the same time, yields more accurate results.

### 2. Linear Segment Method and its Limitations

The complex transfer function of a network may be written

$$Z(p) = \frac{H(p+a_1)(p+a_2)\dots(p+a_k)\dots(p+a_s)}{(p+b_1)(p+b_2)\dots(p+b_m)\dots(p+b_r)} \quad (2)$$

where  $p$  is the complex frequency and the roots of the numerator and the denominator are the zeros and poles respectively of the transfer function  $Z(p)$ . The roots may be real or conjugate complex and, as a result of the minimum phase-shift condition, may lie anywhere in the complex frequency plane to the left of the imaginary axis.

The attenuation-frequency characteristic of the network is obtained by replacing the complex variable  $p$  by  $j\omega$ , so that the magnitude of the resulting complex function gives the output-to-input voltage ratio for the network as a function of the angular frequency  $\omega$ . The attenuation due to the network for frequency  $\omega$  is then given by

$$A(\omega) = 10 \log_{10} e \cdot \log_e |Z(j\omega)|^2 \text{ decibels} \quad (3)$$

It is to be noted that the attenuation due to the network is the sum of a number of logarithms, each of which corresponds to one of the factors of the transfer function.

#### Simple Real Zero or Pole

To understand the application of the method of linear segments in its simplest form we consider first one of the factors  $(p+a)$  of the transfer function  $Z(p)$ . This factor of the transfer function

MS accepted by the Editor, July 1954

can be represented by a simple real zero placed at a distance  $a$  from the origin of the complex plane as depicted in Fig. 1(a). The attenuation characteristic corresponding to this zero is given by

$$A_1(\omega) = 10 \log_{10} (a^2 + \omega^2) \\ = 10 \log_{10} a^2 + 10 \log_{10} (1 + \omega^2/a^2) \quad (4)$$

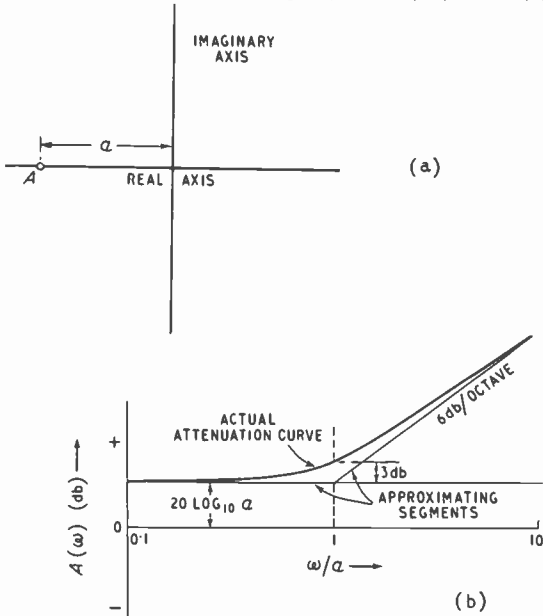


Fig. 1. (a) Simple real zero on the negative real axis and (b) attenuation characteristic and approximating segments corresponding to the real zero of (a). The angular frequency  $\omega$  is normalized with respect to 'a', the distance of the zero from the origin.

Fig. 1(b) shows the plot of this attenuation characteristic on a logarithmic frequency scale. Inspection of the expression for the attenuation characteristic shows that for large values of  $\omega$ , the graph will tend to approximate a straight line, the equation of which is

$$A = 10 \log_{10} \omega^2 \quad \dots \quad (5)$$

The slope of this straight line on the logarithmic plot is approximately six decibels per octave for, if the frequency is doubled, the value of the above expression changes by 6.02. The whole graph may, therefore, be approximately represented by its asymptotic segments which consist of two straight lines, one horizontal, extending from very low values of frequency up to a point  $\omega = a$  and the other inclined to the same and extending from the point  $\omega = a$  up to infinite frequency. This latter segment has been termed a semi-infinite slope. If instead of taking a simple zero a multiple zero were taken, the slope of the graph at a large value of  $\omega$  would have been multiplied by  $n$ ,  $n$  being the multiplicity of the zero.

For the case of a pole instead of a zero we get

similar segments, the only difference being that the slope is negative instead of positive.

With the above, we may now proceed to approximate a given attenuation characteristic by placing a number of straight line segments, horizontal or inclined, running close to the given characteristic in such a way that the slopes of the inclined ones are either 6 db/octave or some multiple of it. Each of the segment junctions then gives the location of a zero or a pole on the real axis in the complex frequency plane. (Zero for the junction for which the slope of the preceding segment is smaller than that of the following, and vice versa.) Hence the straight-line segment representation of the given attenuation characteristic gives the zeros and poles of a transfer function, the attenuation characteristic corresponding to which resembles approximately the given attenuation characteristic.

It is evident, however, that the above method is applicable only to cases in which the attenuation characteristic may be represented closely by segments the slopes of which are restricted to values 6 db/octave or some multiple of the same. As this is not always the case, the method is evidently one of very restricted use.

#### Zero-Pole Pair

Bresler<sup>3</sup> has, however, shown that it is possible to approximate any slope by taking a zero-pole pair instead of a zero or a pole alone, placed

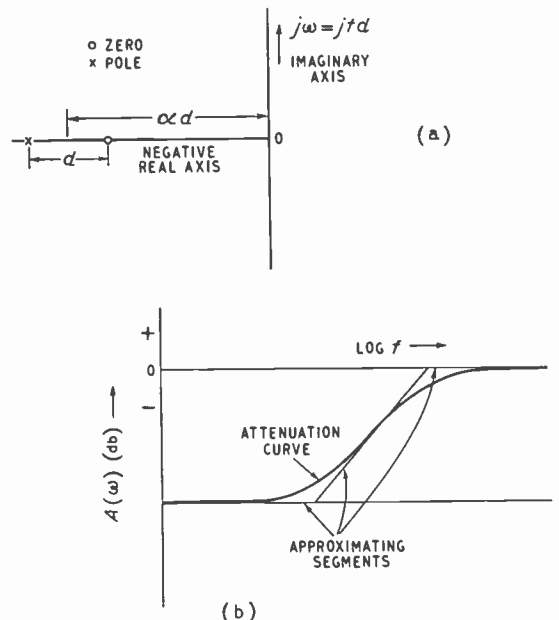


Fig. 2. (a) Bresler's zero-pole pair and (b) attenuation characteristic and approximating segments corresponding to the zero-pole pair of (a);  $f$  is the frequency normalized with respect to the distance 'd' between the poles and zero ( $f = \omega/d$ ).

suitably along the negative real axis of the complex frequency plane as shown in Fig. 2(a). The attenuation characteristic corresponding to these singularities may then be approximated

Fig. 3(a), on a line inclined at an angle  $\theta$  to the real axis and lying in the left half of the complex-frequency plane. The distances in this diagram are normalized by dividing by  $d$ , the distance

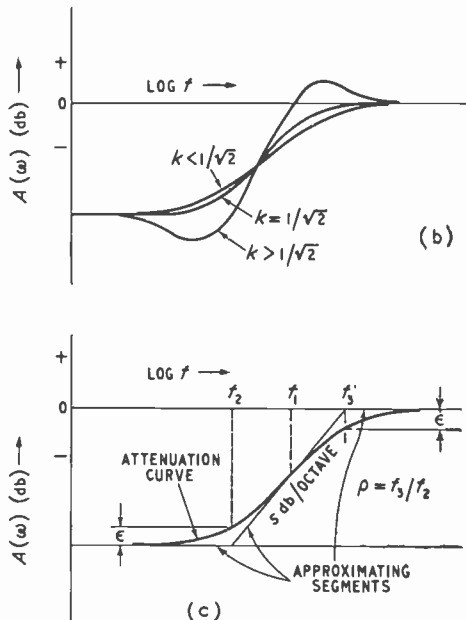
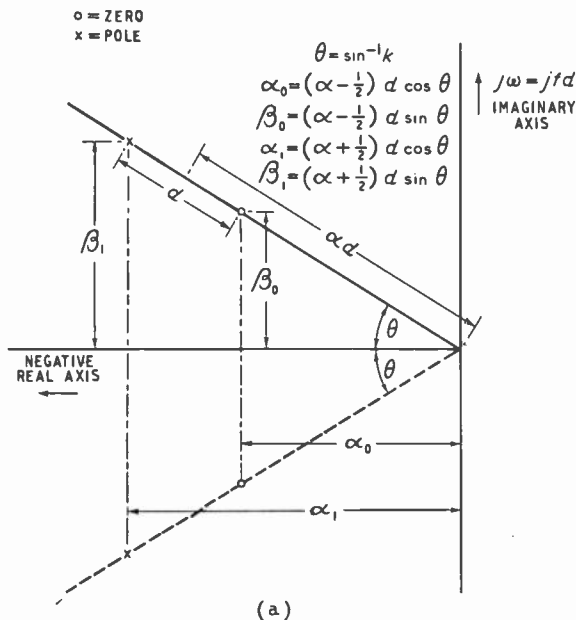


Fig. 3. (a) Zero-pole pair on a line inclined to the real axis; (b) variation of the attenuation characteristic with the value of  $k$ ; and (c) typical attenuation characteristic with approximating segments, corresponding to (a) with  $k < 1/\sqrt{2}$ .

by three linear segments as shown in Fig. 2(b). Unfortunately, the method suffers from a limitation regarding the choice of the length of the middle segment (which is the one to be fitted to the given characteristic). The length must be such that the ratio of the frequencies corresponding to the ends of this segment is eight; i.e., each of the segments chosen must cover a frequency range of three octaves, approximately. This means that variations in attenuation occurring within a frequency range of three octaves cannot be simulated by this method

### 3. Extension of the Linear-Segment Method

The limitation mentioned above, namely, that the length of the middle segment must cover a frequency range of approximately three octaves, can be removed to a great extent if a zero-pole pair is taken on a line inclined to the real axis, the line passing through the origin and lying in the left half of the complex-frequency plane. By changing the slope of this line in the complex-frequency plane, the ratio of the end frequencies may be adjusted over a range of values, the limits of which depend on the slope of the portion of the attenuation characteristic to be approximated. The applicability of the zero-pole arrangement is thus greatly extended.

Consider a zero-pole pair placed, as shown in

between the pole and the zero. This normalization greatly simplifies the expressions.

By referring to Fig. 3(a) the expression for the corresponding transfer function may now be written as

$$Z(p) = \frac{H(p + \alpha_0 + j\beta_0)(p + \alpha_0 - j\beta_0)}{(p + \alpha_1 + j\beta_1)(p + \alpha_1 - j\beta_1)} \quad (6)$$

It may be noted that any network which has the same singularities as shown in Fig. 3(a) has a transfer function which differs from (6) by a constant multiplier only. Since this constant multiplier can be introduced very easily and, since it does not affect the nature of the attenuation function, but simply moves it bodily upwards or downwards, the constant will henceforth be omitted.

The attenuation characteristic corresponding to  $Z(p)$  is at once written down from (6) as

$$A_2(\omega) = 10 \log_{10} \frac{[f^2 + (\alpha - \frac{1}{2})^2]^2 - 4f^2k^2(\alpha - \frac{1}{2})^2}{[f^2 + (\alpha + \frac{1}{2})^2]^2 - 4f^2k^2(\alpha + \frac{1}{2})^2} \quad (7)$$

Plots of this function on a logarithmic frequency scale are shown in Fig. 3(b) for different values of  $k$ . It is seen that all the curves start from the same level on the low-frequency end and reach the same final level at the high-frequency end. In the intermediate region the attenuation

characteristic follows a path that depends on the value of  $k$  ( $= \sin \theta$ ). If we draw a tangent to any of the graphs at its point of inflexion (which point may be shown to be the point where the attenuation is midway between the initial and the final values), and produce it in either direction so that it crosses the initial and the final levels, the resulting straight-line segment, together with the horizontal portions at the low- and high-frequency ends, approximate the attenuation characteristic corresponding to the zero-pole pair taken. [See Fig. 3(c)]. We thus obtain a set of three straight-line segments in the form of a framework, so to say, to represent the attenuation characteristic corresponding to the complex zero-pole pair being studied. It is our object to use such frameworks, as convenient units, for approximating any given attenuation characteristic.

As in the case of Bresler's zero-pole pair, the attenuation characteristic is again representable by three straight-line segments; but here the restriction that the end frequency ratio of the central inclined segment is to be nearly eight no longer exists. There appears, however, another restriction. The attenuation characteristics of the form shown in Fig. 3(b)—with which we intend to represent approximately the different portions of a given characteristic—develop humps when the value of  $k$  is greater than about  $1/\sqrt{2}$ . Obviously, curves with such humps are unsuited for our approximation purpose. To avoid curves with humps the allowable inclination of the line on which the zero-pole pair lies has to be so restricted that  $\theta$  is less than  $\sin^{-1}(1/\sqrt{2})$ . This, in other words, means that the zero-pole pair chosen should lie on a line with inclination to the real axis limited between  $0^\circ$  and about  $45^\circ$ . This limitation in the value of  $k$  necessarily sets certain limits to the admissible values of the end frequency ratio  $\rho$  of the central segment and, also the slope  $S$  of the same. These limits are as follows:

$$\rho_1 \leq \rho \leq \rho_2 \dots \dots \dots (8)$$

$$\text{where } \rho_1 = \left[ \frac{6}{S} + \sqrt{\left(\frac{36}{S^2} - \frac{1}{4}\right)} + \frac{1}{2} \right]^{12/S} \dots \dots \dots (9)$$

$$\text{and } \rho_2 = \left[ \frac{6 + S/2}{6 - S/2} \right]^{12/S} \dots \dots \dots (10)$$

$$\text{also, } S \leq 12 \text{ decibels/octave} \dots \dots \dots (11)$$

The limiting values of  $\rho$  are plotted in Fig. 6. (Proofs of the derivation of these limits are given in the Appendix.)

In approximating a given attenuation characteristic by means of straight-line segments, the given curve is divided into a number of sections

in a suitable manner, and for each of these sections one linear segment is taken. It may so happen that some of the segments will not have their slopes or end frequency ratios within the limits specified above. If the end frequency ratio is greater than the maximum allowed value for the slope to be approximated, the section may be broken up into smaller ones. If, on the other hand, the value of  $\rho$  falls below the minimum allowable value for the given slope, the section may be considered as composed of two sections with opposite slopes, placed suitably along the frequency axis. In order to avoid such complications, a straightforward method of adjustment of the segments is adopted. This is given in Section 5, and illustrated in Section 7.

It is important to remember that in the calculation of the transient response from the transfer function, the evaluation of the residues corresponding to the assumed poles is necessary. For the case of multiple poles this requires the differentiation of the transfer function with respect to  $p$ . This may make the actual computation lengthy, specially if the number of singularities is large. For the simple pole, however, the calculation of the residue is easy. It is desirable therefore, that the assumption of multiple poles be avoided so far as practicable. Thus if a slope greater than 12 decibels per octave is to be approximated, the slope is divided into a number of unequal parts the sum of which is equal to the given slope. Evidently, the zero-pole pairs obtained in this way are all simple.

#### 4. Attenuation Error

Before the calculation of the location of the zeros and poles corresponding to the assumed segments is undertaken, the approximate attenuation characteristic should be compared with the given characteristic to estimate what may be called the 'attenuation error'; i.e., the departure of the assumed attenuation characteristic (the one represented by the linear segments) from the characteristic to be simulated.

It is clear from Fig. 3(c) that the departure of a point on an approximating linear segment from the corresponding point on the attenuation characteristic represented by the segment is a maximum at the ends of the segment. It is therefore enough to compare these end departures ( $= \epsilon$ ) with the actual departures of the ends of the segments from the given characteristic to get an idea of the attenuation error. In order to facilitate the comparison, graphs of  $\epsilon$  are plotted for different values of  $\rho$  and  $S$ . (Fig. 7.) For any tentative choice of the segments the attenuation-error values at the ends of the segments are noted from the plot. If the error at any point is found to be very large, one or two of the segments

are adjusted suitably (with the help of the graphs in Fig. 7) to minimize the error.

### 5. Choice and Adjustment of the Linear Segments

The attenuation-frequency characteristic for any actual network has a constant limiting slope at its two ends; that is, both for very high and for very low frequencies. It can be shown that this limiting slope must be either zero or some multiple of six decibels, approximately, per octave. The limiting slopes may, therefore, be approximated by real zeros or poles, simple or multiple. The value of  $\epsilon$  for a simple zero is +3 db, and that for a simple pole is -3 db; for a zero or pole of multiplicity  $n$ , these are +3 $n$  db and -3 $n$  db respectively. For zero-pole pairs,  $\epsilon$  is positive at the low-frequency end and negative at the high-frequency end for a segment with positive slope and, vice versa. The  $\epsilon$  values for zero-pole pairs are plotted in Fig. 7.

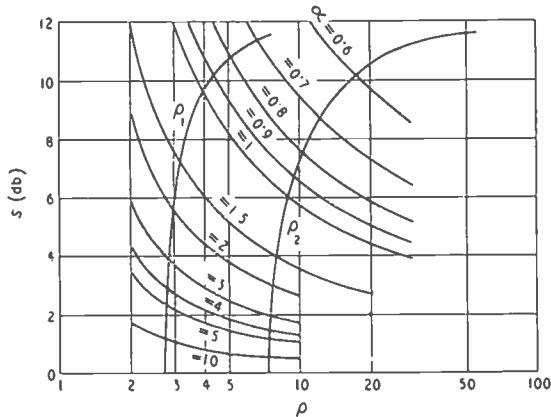


Fig. 4. Plot of  $S$  against  $\rho$  for different values of  $\alpha$ .

The straight-line segments are chosen in such a way that they are approximately tangential to the given characteristic. The segment lengths are adjusted successively so that the sum of the  $\epsilon$  values of the adjacent segments equals the distance of the junction of the segments from the given characteristic. This means that the attenuation errors at the segment ends are zero. (The procedure is explained in detail in an illustrative example to follow.)

The closeness of approximation of the attenuation characteristic determines the closeness with which all the other characteristics are approximated. This is so, because, as has already been pointed out, for one attenuation characteristic realized in minimum phase-shift form, there exists one and only one phase-shift characteristic. Hence, in working out an actual problem, it is helpful to remember that the larger the number of segments taken and the smaller the attenuation

errors at the ends of the segments, the better is the approximation.

### 6. Calculation of Transient Response: Location of Singularities

Once the choice of the segments is completed, the locations of the singularities corresponding to these segments are found with the help of the graphs in Figs. 4 and 5, or by direct calculation from the relations (16), (20) and (21) given in the Appendix. When the graphs are used,  $\alpha$  is found from  $S$  and  $\rho$  in Fig. 4, and  $k$  from  $\alpha$  and  $S$  in Fig. 5. Knowing  $\omega_1$ , the geometric mean angular frequency of the segment,  $d$  is calculated from relation (16) given in the Appendix. The complex transfer function approximately representing the given attenuation characteristic is then written down at once, without the constant  $H$ , which is still to be evaluated. For calculating  $H$  we write out the expression

$$\frac{(p + \alpha_0 + j\beta_0)(p + \alpha_0 - j\beta_0) \dots}{(p + \alpha_1 + j\beta_1)(p + \alpha_1 - j\beta_1) \dots} \quad (12)$$

Here  $\alpha_0, \beta_0$ , etc. are the real and imaginary components of the calculated zero locations, and  $\alpha_1, \beta_1$ , etc. are the same quantities for the pole locations. The function (12) corresponds to the given attenuation characteristic with only the constant  $H$  missing. This means that, if the magnitude of the function (12) is plotted against a logarithmic frequency scale, the resulting curve will differ from the given attenuation characteristic at all points by a constant gain or loss of value  $H$ . To obtain  $H$ , therefore,  $p$  in expression (12) is given a pure imaginary value  $j\omega$  and the magnitude of the expression calculated.

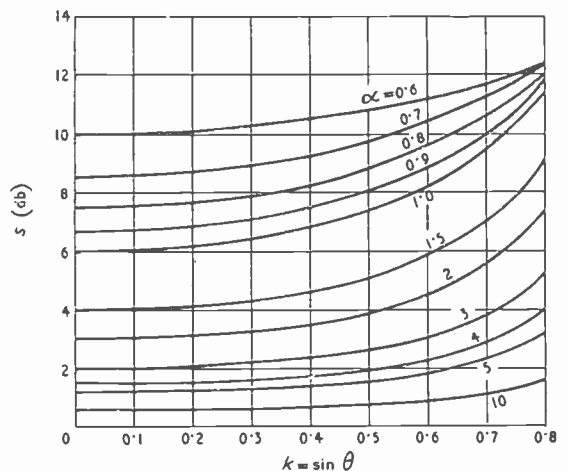


Fig. 5. Plot of  $S$  against  $k$  for different values of  $\alpha$ .

The ratio of the magnitude of the given plot of  $A(\omega)$  to this calculated magnitude at the same frequency is the required factor  $H$ . For the

special cases in which the initial or the final value of the slope of the given attenuation characteristic is zero, the calculations are obviously simplified if  $p$  is taken to be equal to zero and infinity respectively.

After  $H$  is obtained, the approximate transfer function is known completely, and the transient response is calculated by the operational method.

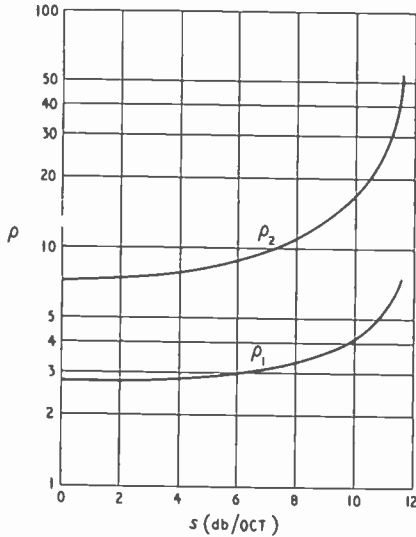
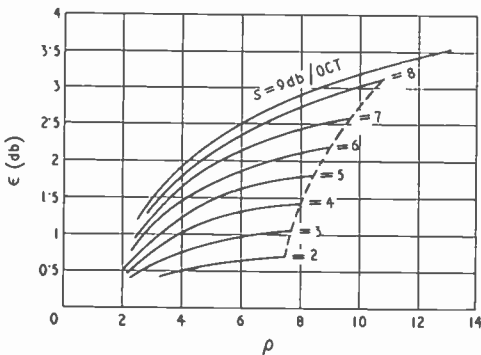


Fig. 6 (above). Limits of  $\rho$  for different values of  $S$ .

Fig. 7 (below). Plot of  $\epsilon$  against  $\rho$  for different values of  $S$ .

Fig. 8 (right). Approximating a given attenuation characteristic by linear segments.



## 7. Example

To illustrate the method of linear segments as extended by us we shall consider a system of which the attenuation characteristic and the corresponding transfer function are known. The curve in Fig. 8, is a plot of the attenuation characteristic of a system whose transfer function is

$$Z(p) = 8.33 \frac{(p+1)(p+20)}{(p+3.33)(p+5)(p+10)} \dots \quad (13)$$

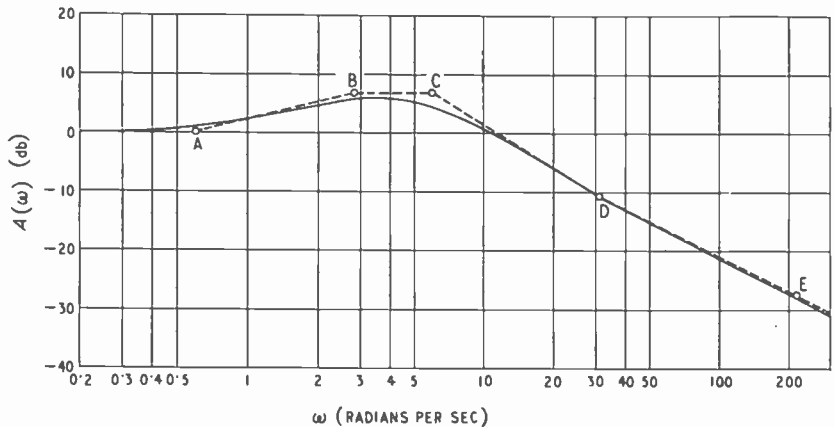
The attenuation characteristic shown in Fig. 8 is thus a plot of

$$A(\omega) = 10 \log_{10} \frac{(1+\omega^2)(1+\omega^2/400)}{(1+\omega^2/11.1)(1+\omega^2/25)(1+\omega^2/100)} \dots \quad (14)$$

We shall calculate the response of this system to Dirac's  $\delta$  function, first, from the attenuation characteristic in Fig. 8 by the linear segment method, and then, directly from (13) by the conventional operational method. The two results will then be compared to judge the accuracy of the method.

### Calculation by the Method of Linear Segments

The first step is to select the straight-line segments to represent approximately the graph



of  $A(\omega)$  as shown in Fig. 8. The selections are made as follows:—

First, the initial (i.e., low-frequency) slope is drawn. This, in the example chosen, is the frequency axis itself; i.e., the slope  $S = 0$ . The point A on the frequency axis from which the second segment is drawn, is next chosen. The choice is somewhat arbitrary, it being only observed that the point is not too far from the corresponding point on the given characteristic. Thus, the  $\epsilon$  value of the first segment being zero (since  $S = 0$ ), that of the second segment alone is to be made equal to the distance of the point A

from the given characteristic, in order that the attenuation error at the point A may be zero; the point A is accordingly chosen such that the slope of the tangent drawn from it to the given characteristic allows a value of  $\epsilon$  larger than the distance of A from the given characteristic.

As actually chosen, the distance of A from the given characteristic is about 1 db, while the slope of the tangent AB is 3 db/octave which, from Fig. 7, allows a maximum value of  $\epsilon$  equal to 1.05 db nearly. To fix the length AB we note from Fig. 7 that for the slope  $S = 3$  db/octave and  $\epsilon = 1$  db, the ratio  $\rho$  of the frequencies at B and A should be 4.67 nearly. Hence, the point B is so chosen that the frequency there is 4.67 times that at A. We note that the distance of the point B from the corresponding point on the graph is very nearly 1 db. Hence, the attenuation error at B would be zero if the next segment from B were horizontal. (This is a mere coincidence. As a matter of fact, if the point A were chosen at some higher or lower frequency, the third segment would not have been horizontal. Horizontal segments are, however, always preferable to sloping segments, for such segments may be given any end frequency ratio conveniently.) The third horizontal segment is then drawn and its length (that is, the point C) is chosen in a manner similar to that for the case of the point A. The fourth segment CD, drawn tangent to the given characteristic, is found to have a slope of 7.38 db/octavenearly. This allows a maximum value of  $\epsilon$  equal to 2.8 db, and the departure of C from the given characteristic ( $= 2.25$  db) is less than this. The end point D of the tangent CD is fixed by noting, from Fig. 7, that for a slope  $S=7.38$  db/octave and for  $\epsilon = 2.25$  db, the required value of  $\rho$  is 5.17, so that D is taken at a point where the frequency is 5.17 times that at C. The length of the fourth segment drawn from C is thus fixed and the point D is obtained. The fifth segment DE is drawn as a tangent to the given characteristic from D. The slope is measured to be 6 db/octave. Now, the  $\epsilon$  value for CD is 2.25 db and the distance of D from the characteristic is  $- 0.25$  db; hence, the  $\epsilon$  value for DE must be equal to the sum of the two; i.e., equal to 2 db.

This is obtained approximately by taking the  $\rho$  value for DE as 7.0. This fixes the point E. The final slope being 6 db/octave, a simple real pole is introduced at E. The  $\epsilon$  value for this real pole is  $- 3$  db. As the distance of the point from the curve is only about 0.5 db, the attenuation error at E is  $(3 - 2.5 =) 0.5$  db nearly. This may be tolerated, because at E the attenuation is already rather large, and a small difference in this region, or at still higher frequencies, would not affect the transient response materially.

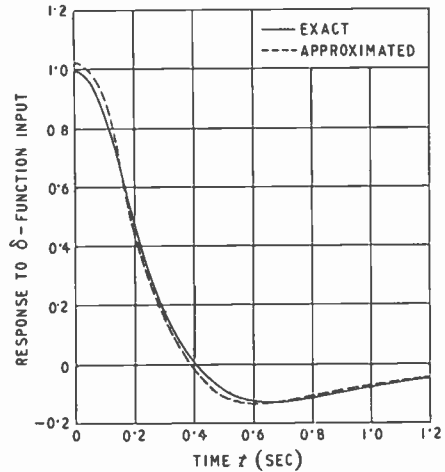


Fig. 9. Exact and approximated response to  $\delta$ -function input.

TABLE 1

Segment	S (db/oct)	$\rho$	Geometric mean freq. of segment ends (radians/sec)	$\alpha$	$h$	$d$	Nature and Location of calculated Zeros and Poles
AB	3.00	4.67	1.3	2.63	0.500	0.504	Poles at $- 1.367 \pm j0.69$ Zeros at $- 0.928 \pm j0.536$
CD	7.38	5.17	13.8	1.07	0.557	14.51	Poles at $- 6.9 \pm j4.625$ Zeros at $- 18.94 \pm j12.7$
DE	6.0	7.0	81.0	1.11	0.354	81.8	Poles at $- 46.6 \pm j17.65$ Zeros at $- 123.2 \pm j46.6$
E to $\infty$	6.0						Pole at $- 217 \pm j0$

In order to calculate  $H$ , the point  $p = 0$  is chosen since the initial slope of the characteristic is zero.  $H$  is then found to be equal to 8.85.

The calculated singularities are shown in the table and the transient response curve of the system having these singularities is shown by the broken line curve in Fig. 9. The exact response curve of the system as calculated directly from the singularities in the expression (13) is shown by the solid-line curve. The agreement between the two is surprisingly good.

### 8. Conclusion

The extension of the linear-segment method, by the utilization of zero-pole pairs lying on a line inclined to the real axis, is found to be quite suited for practical calculations. The whole improvement depends on the fact that the lengths and the slopes of the approximating segments are less restricted. This is to be expected, because, in the previous methods mentioned in the text the singularities are restricted to lie on a single line in the complex plane, while in the method described here there is much greater freedom in the location of the zeros and the poles.

An obvious generalization of the method would be to place a zero and a pole on two separate lines passing through the origin in the left half of the complex plane, and having different slopes. But a study of this arrangement shows that it makes the calculations more complicated and the fitting more difficult.

### Acknowledgments

The author is deeply indebted to Prof. S. K. Mitra for his kind interest in the work and to Mr. Arun K. Chowdhury, M.Sc. for constant help and guidance. Thanks are also due to Mr. Nirmal B. Chakraverty for some helpful discussions. He is grateful to the Ministry of Education, Government of India, for the award of a Scholarship.

### APPENDIX

To find the slope ( $S$ ) of the attenuation characteristic corresponding to a chosen zero-pole pair at the point of inflexion we first note that this point is given by the equation

$$A_2(\omega) = 10 \log_{10} \left[ \frac{\alpha - \frac{1}{2}}{\alpha + \frac{1}{2}} \right]^2 \quad \dots \quad (15)$$

and hence, solving the equation,

$$f_1 = \sqrt{\alpha^2 - \frac{1}{4}} = \frac{\omega_1}{d} \quad \dots \quad (16)$$

$S$  is then obtained by differentiating expression (7) with

respect to  $\log f$ , and substituting the value of  $f_1$  in the resulting expression. Thus

$$S = \frac{20 \alpha}{\alpha^2 - \frac{1}{4}} \text{ db/octave} \quad \dots \quad (17)$$

$S$  is plotted against  $k$  for different values of  $\alpha$  in Fig. 5.

The end frequency ratio ( $\rho$ ) is now calculated as the frequency ratio required to produce a change in the attenuation of

$$20 \log \left[ \frac{\alpha - \frac{1}{2}}{\alpha + \frac{1}{2}} \right]^2 \text{ decibels for a slope } S.$$

This comes out to be

$$\rho = \frac{f_3}{f_2} = \left[ \frac{\alpha + \frac{1}{2}}{\alpha - \frac{1}{2}} \right]^{12/S} \quad \dots \quad (18)$$

$S$  is plotted against  $\rho$  for different values of  $\alpha$  in Fig. 4. From Fig. 3(c) it is also clear that the relation

$$f_1^2 = f_2 \cdot f_3 \quad \dots \quad (19)$$

holds.

Equations (17) and (18) may be solved for  $\alpha$  and  $k$ ; the solutions are:

$$\alpha = \frac{1}{2} \cdot \frac{\rho S / 12 + 1}{\rho S / 12 - 1} \quad \dots \quad (20)$$

$$k = \left[ \frac{S \alpha^2 - 6 \alpha}{S (\alpha^2 - 1/4)} \right]^{1/2} \quad \dots \quad (21)$$

Now, in order that the values of  $\rho$  and  $S$  taken may correspond to a zero-pole pair lying within  $0^\circ$  and  $45^\circ$ , the condition

$$0 \leq k \leq \frac{1}{\sqrt{2}} \quad \dots \quad (22)$$

must be satisfied. The condition restricting the complex zero-pole pair to lie within the region between  $0^\circ$  and  $45^\circ$  in the left-half plane, imposes a corresponding restriction on the maximum allowable value of the slope of the middle segment, and also restricts the frequency ratio  $\rho$  within certain limits, these limits depending on the value of  $S$ . From (21) and (22) we obtain:

$$\frac{6}{S} \leq \alpha \leq \frac{6}{S} + \left( \frac{36}{S^2} - \frac{1}{4} \right)^{1/2} \quad \dots \quad (23)$$

Again, from (20) and (23) we may write

$$\rho_1 \leq \rho \leq \rho_2 \quad \dots \quad (8)$$

where

$$\rho_1 = \left[ \frac{6/S + (36/S^2 - 1/4)^{1/2} + \frac{1}{2}}{6/S - (36/S^2 - 1/4)^{1/2} - \frac{1}{2}} \right]^{12/S} \quad \dots \quad (9)$$

and

$$\rho_2 = \left[ \frac{6 + S/2}{6 - S/2} \right]^{12/S} \quad \dots \quad (10)$$

From the relation (23) it is also clear that  $S$  must be less than 12 decibels per octave.

### REFERENCES

- <sup>1</sup> H. W. Bode, "Network Analysis and Feedback Amplifier Design", D. Van Nostrand & Co.
- <sup>2</sup> O. P. D. Cutteridge, "A Graphical Contribution to the Analysis and Synthesis of Electrical Networks", *Proc. Instn elect. Engrs*, Part IV, October 1953.
- <sup>3</sup> A. D. Bresler, "On the Approximation Problem", *Proc. Inst. Radio Engrs*, December 1952.
- <sup>4</sup> R. F. Baum, "A Contribution to the Approximation Problem", *Proc. Inst. Radio Engrs*, 1948, Vol. 36, p. 863.
- <sup>5</sup> J. M. Linke, "A Graphical Approach to the Synthesis of General Insertion Attenuation Functions", *Proc. Instn elect. Engrs*, Part III, 1950, p. 179-187.

# AUTOMATIC SLIDE-BACK VOLTMETER

## Peak Reading on Positive Pulses

By Herbert J. Fraser, A.M.I.E.E.

(Amalgamated Wireless Valve Co. Pty. Ltd., Sydney, Australia)

**SUMMARY.**—An automatic slide-back voltmeter designed to indicate directly the peak voltage of recurring positive pulses is described. The voltage to be measured is applied to a diode detector which is automatically biased so that the difference between the input voltage and the slide-back bias is small. The slide-back bias is obtained by integrating the output pulses of a multivibrator which is triggered by this difference voltage. The voltmeter can be calibrated from a d.c. source.

Experimental results are given which cover the range of pulse widths 0.5–50  $\mu$ sec and pulse repetition rates 10–20,000 c.s. The maximum error is  $\pm 2$  volts over the range 0–100 volts.

### 1. Introduction

RADIO valves are tested under recurring pulse conditions to obtain emission and static characteristics under conditions of class C or pulse operation, while keeping the average power dissipated in the valves within rated limits. The large quantities of different types of valves handled in production require a direct-reading instrument to measure the amplitudes of the voltage and current pulses over a wide range of pulse duty cycles. Such an instrument suitable for incorporation in a production test set is described. Several types of direct-reading instruments were considered and rejected for the following reasons.

The diode peak-reading voltmeter with d.c. amplifier is unsatisfactory at very low duty cycles because of the extremely high values of resistance needed in the diode load and amplifier input circuit.

Pulses are commonly measured on a cathode-ray oscilloscope calibrated by d.c. shift, but this method is considered too expensive and too complex for a production test set where servicing time must be minimized.

The automatic slide-back voltmeter described by Creveling and Mautner<sup>1</sup> is satisfactory for the purpose but it requires a cathode-ray oscilloscope for calibration and its operation is restricted to the duty cycle range of approximately  $10^{-3}$  to 4%.

The voltmeter to be described is an automatic slide-back type which can be calibrated from a d.c. source. It is a direct-reading instrument which covers the duty cycle range of  $5 \times 10^{-4}$  to 100% and it has the further advantage that, because no high-gain amplifiers are used, the problems of hum pickup and instability are avoided.

### 2. Description of Basic Circuit

The voltmeter is represented by the simplified circuit of Fig. 1. When the input voltage  $E_{in}$

exceeds the feedback bias  $E$  the diode  $V_1$  conducts and a voltage is developed across the diode load resistor  $R_1$ . This voltage triggers a multivibrator which gives an output pulse of essentially constant width and amplitude each time it is triggered. The output pulses are integrated to obtain a steady unidirectional voltage which is fed back as bias to the diode in the correct direction to reduce its conduction. The feedback bias automatically increases with input voltage to maintain the multivibrator near its triggering level  $E_I$  and it is therefore a direct measure of input voltage minus  $E_I$ . The necessary variation in feedback bias required over the

range of input voltage to be measured is obtained by automatic variation of the triggering rate of the multivibrator.

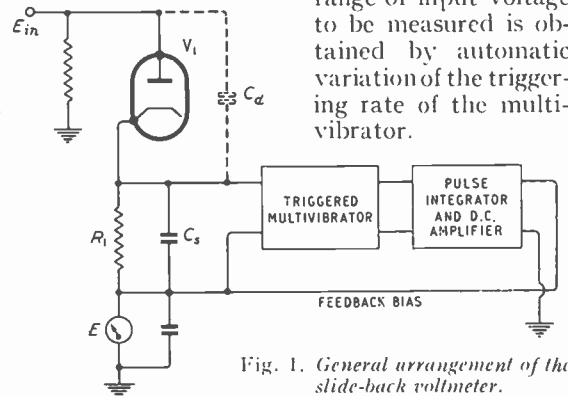


Fig. 1. General arrangement of the slide-back voltmeter.

Factors which affect the reading of the voltmeter are:

- (a) Voltage directly fed through the anode-to-cathode capacitance  $C_d$  of the diode.
- (b) Voltage required to trigger the multivibrator.
- (c) Diode contact potential.
- (d) Voltage drop across the diode.
- (e) Input pulse width and repetition rate.
- (f) Needle flicker in the meter due to irregularity or ripple in the feedback bias.

These factors will be discussed in this order.

The shunt capacitance  $C_s$  is added to reduce the voltage fed through the diode capacitance

MS accepted by the Editor, July 1954

$C_d$  to

$$E_{in} \cdot \frac{C_d}{C_s + C_d} \text{ volts.}$$

Provided this voltage is below the triggering level of the multivibrator it results in an error equal only to its own magnitude. In order to keep  $C_s$  small and so obtain low capacitive input loading the multivibrator is biased one volt below its triggering level.  $C_s$  is made 100 times greater

With high duty cycles the voltage developed across  $R_1 C_s$  does not decay completely between pulses but, because the d.c. component across  $R_1 C_s$  is an effective part of the triggering voltage, no error results.

The amount of needle flicker in the meter due to ripple in the feedback bias can be reduced by design at the expense of response time. This problem is discussed in the next section.

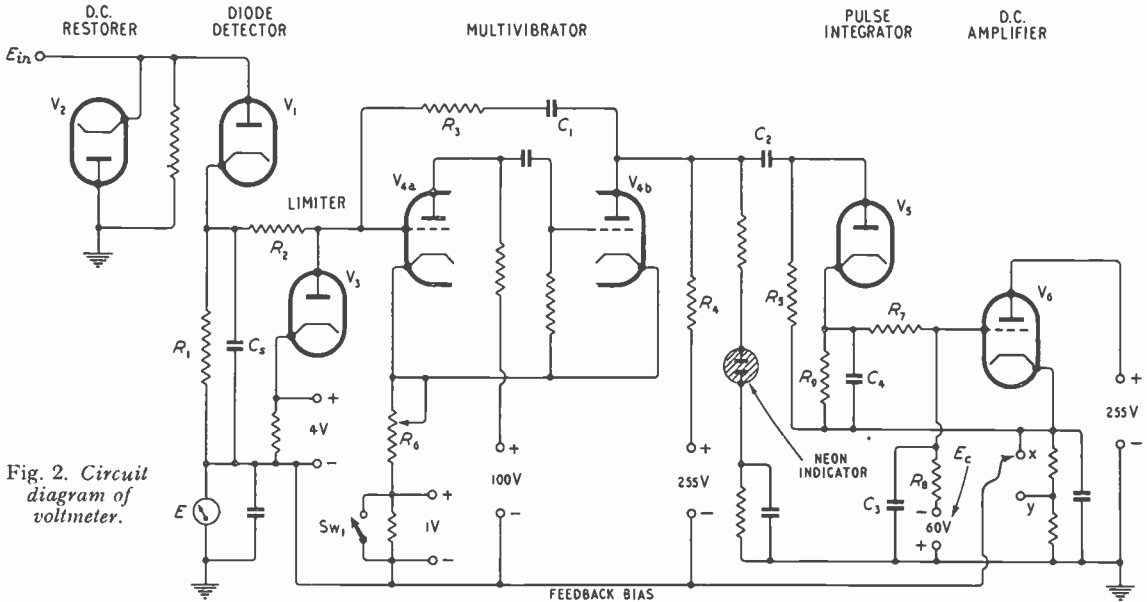


Fig. 2. Circuit diagram of voltmeter.

than  $C_d$  and therefore the instrument can measure input voltages up to 100 volts before capacitive feed through  $C_d$  is sufficient to trigger the multivibrator. The error due to  $C_d$  is thus reduced by  $C_s$  to + 1% and because the multivibrator is biased one volt below its triggering level it is inherently stable and insensitive to extraneously induced voltages. The error due to this bias on the multivibrator can be eliminated by a constant additive correction of + one volt.

Diode contact potential, which is usually of the order of 0.7 volt, can be completely cancelled by suitably biasing the diode although this has not been done in the present instrument.

The voltage drop across the diode anode resistance  $r_a$  is equal to  $E_t r_a / R_1$  volts, which can be neglected as  $R_1 > 500 r_a$ .

Provided that the input pulses are sufficiently wide to trigger the multivibrator, the limit to low duty-cycle measurements occurs at low pulse-repetition rates because the integrator and d.c. amplifier cannot maintain sufficient feedback bias if the multivibrator is not triggered often enough. This design problem is discussed later.

### 3. Complete Circuit and Experimental Results

The circuit of the voltmeter in its final form is shown in Fig. 2.

The diode  $V_2$  operates as a d.c. restorer so that any capacitance in series with the input source which is charged by conduction of  $V_1$  will be discharged by  $V_2$  between pulses and will not affect the accuracy of the measurement.

Diode  $V_3$  in conjunction with the resistor  $R_2$  limits the input pulse amplitude to the multivibrator grid to four volts as it was found by experiment that triggering would not occur for an input greater than eight volts. In normal operation ( $V_3$  non-conducting) the voltage drop which occurs across  $R_2$  results in an error of

$$- E_t \left[ \frac{R_2 + R_3}{R_3} \cdot \frac{1}{1 - \exp. - \left( \frac{t}{R_2 C_{in}} \cdot \frac{R_2 + R_3}{R_3} \right)} - 1 \right] \text{ volts}$$

where  $C_{in}$  = input capacitance of  $V_3$  and  $V_{4a}$   
 $t$  = pulse-width (seconds)  
 $C_1, R_4, R_5$ , are neglected as their impedances are much less than  $R_3$ . This error is equal to - 0.2

volt at large pulse width and increases to  $-0.26$  volt for an input pulse width of  $0.5 \mu\text{sec}$ . If the pulse generator coupled to the voltmeter has sufficient internal impedance  $R_2$  may be zero and this error eliminated.

The multivibrator circuit has two feedback paths. Because the common cathode resistor  $R_6$  must be relatively small to satisfy other design requirements, a second feedback path is obtained through  $R_3C_1$  connected from the output anode to the input grid to ensure that reliable self-oscillation of the multivibrator can be obtained.

The method of setting the multivibrator one volt below its triggering level is to decrease  $R_6$  until self-oscillation is detected by the neon indicator and then switch one volt bias obtained from a regulated supply into the circuit by the switch  $SW_1$ .

Experimental work has shown that the self-oscillating condition reached in the above way corresponds to the triggering point to within  $\pm 0.1$  volt.

The d.c. amplifier  $V_6$  allows measurement of the feedback bias on a 1,000-ohms per volt meter. In the absence of any input signal  $V_6$  is biased to cut-off. An input signal produces multivibrator pulses which are integrated into the capacitor  $C_3$  to raise  $V_6$  above cut-off to supply the correct feedback bias.

In order to explain the action of the integrating circuit let the duration of the multivibrator output pulse be  $t_p$  second and its amplitude  $E$  volts. The capacitor  $C_4$  is charged by each

where  $t_2$  = time between multivibrator output pulses

$E_0$  = Voltage on  $C_3$ , which is approximately equal to the feedback voltage

$E_c$  = Bias supply for  $V_6$

The net voltage gained by  $C_3$  per pulse is then

$$\Delta E_{c3} = \frac{EC_2}{C_4 + C_2} \cdot \frac{C_4}{C_3} - (E_0 + E_c) \left[ 1 - \exp\left(\frac{-t_2}{R_8 C_3}\right) \right] \text{ volts}$$

The circuit is designed so that the maximum value of  $E_0$  (100 volts) is obtained for the value of  $t_2$  (0.1 sec) corresponding to the minimum pulse rate (10 c/s). If  $E$ ,  $E_0$ ,  $C_2$  and  $t_2$  are fixed it can be seen that  $C_4/C_3$  and  $R_8 C_3$  must be sufficiently large to obtain a net voltage increase on  $C_3$  per pulse and so allow the feedback bias to rise. If  $\Delta E_{c3}$  is large, the response time is small but the ripple in the feedback bias is large. The time  $t_s$  required fully to establish the feedback bias  $E_0$  at a pulse rate of  $n$  c/s is given by

$$t_s = \frac{E_0}{n \cdot \Delta E_{c3(av)}} \text{ seconds}$$

where  $\Delta E_{c3(av)}$  is the average value of  $\Delta E_{c3}$  over the time  $t_s$ . In the present circuit  $\Delta E_{c3(av)} =$  two volts, hence a time of five seconds is required to establish 100 volts feedback bias at the lowest input pulse repetition rate of 10 c/s. The percentage ripple in the feedback bias equals  $100 \Delta E_{c3}/E_0$ . As  $\Delta E_{c3}$  is fixed this becomes more serious for low values of  $E_0$ . This ripple can be reduced at low voltage by obtaining the feedback bias across part of the cathode load on  $V_6$  by switching the feedback bias line from X to Y of

Fig. 2 but this also proportionately decreases the amplitude range of the voltmeter.

Experimental results obtained with the circuit of Fig. 2 are shown in Fig. 3.

Pulse amplitudes were checked to  $\pm 2\%$  by a pulse c.r.o. calibrated by d.c. shift.

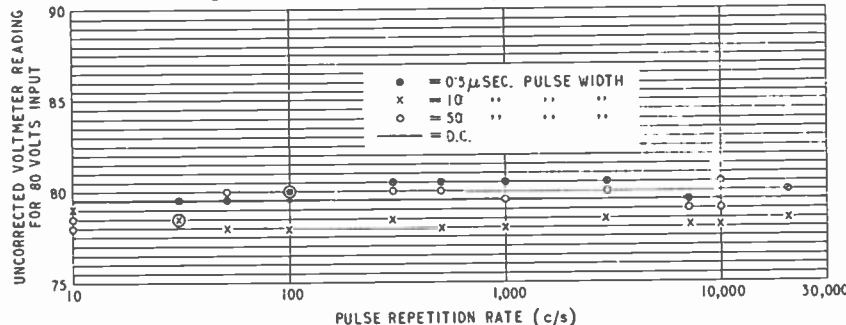


Fig. 3. Measured performance for various kinds of input.

pulse to a peak value of  $EC_2/(C_2 + C_4)$  volts and then  $C_4$  discharges through  $R_7$  into  $C_3$  ( $C_3 \gg C_4$ ) thus increasing the voltage across  $C_3$  for each pulse by the amount

$$+ \Delta E_{c3} = E \cdot \frac{C_2}{C_4 + C_2} \cdot \frac{C_4}{C_3} \text{ volts}$$

The discharge through  $R_9$  can be neglected as  $R_9 \gg R_7$  and the charge entering  $C_3$  during the pulse time  $t_p$  is negligible as  $t_p \ll R_7 C_3$ . Between pulses  $C_3$  discharges through  $R_8$  by the amount

$$- \Delta E_{c3} = (E_0 + E_c) \left[ 1 - \exp\left(\frac{-t_2}{R_8 C_3}\right) \right] \text{ volts}$$

### Acknowledgments

The author wishes to thank Mr. D. Stace who assisted in the development of the voltmeter, carried out all the constructional work and obtained the experimental results.

Thanks are due to Amalgamated Wireless Valve Co. Pty. Ltd. for permission to publish this paper.

### REFERENCE

<sup>1</sup> "An Automatic Slideback Peak Voltmeter for Measuring Pulses", C. J. Creveling & L. Mautner, *Proc. Inst. Radio Engrs*, February 1947, p. 208-211.

# MATRIX ALGEBRA

## Special Applications to Four-Poles

By John J. Karakash

**SUMMARY.**—Matrix algebra has been applied to electrical-circuit theory with considerable success. Impedance and admittance matrices are frequently employed to formalize general solutions of some network problems; similarly, the scattering matrix formalizes solutions of problems in terms of reflection coefficients in microwave multi-terminal structures. This paper\* deals with special procedures and applications involving the general parameter matrix of passive four-poles with bilateral circuit elements.

### 1. General Parameter Matrix

It is known that the general parameter matrix with elements  $A, B, C, D$ , relates the external conditions of four-poles (Fig. 1) in the manner

$$\begin{bmatrix} E_s \\ I_s \end{bmatrix} = \begin{bmatrix} A & B \\ C & D \end{bmatrix} \begin{bmatrix} E_L \\ I_L \end{bmatrix} \quad \dots \quad (1)$$

the linear relations being written in algebraic form

$$\left. \begin{aligned} E_s &= AE_L + BI_L \\ I_s &= CE_L + DI_L \end{aligned} \right\} \quad \dots \quad (2)$$

The elements of the square matrix in (1) can be determined through open-circuit or short-circuit measurements or in terms of the internal mesh determinant of the four-pole. Referring to a four-pole with a mesh determinant of the  $n$ th order, a pair of input terminals ( $1-1$ ) and a pair of output terminals ( $n-n$ ), the elements of the square matrix in (1) are given by

$$\begin{aligned} A &= M_{nn}/M_{1n}; & B &= D_n/M_{1n}; \\ C &= M_{11n}/M_{1n}; & D &= M_{11}/M_{1n} \end{aligned} \quad \dots \quad (3)$$

where  $D_n$  is the mesh impedance determinant of the four-pole and the  $M$  terms the appropriate co-factors. Thus, if the four-pole has  $n$  meshes and consists of passive, linear circuit elements,

$$D_n = \begin{vmatrix} z_{11} & z_{12} & \dots & z_{1,n-1} & z_{1n} \\ z_{21} & z_{22} & \dots & z_{2,n-1} & z_{2n} \\ \vdots & \vdots & \ddots & \vdots & \vdots \\ z_{n-1,1} & \dots & \dots & z_{n-1,n-1} & z_{n-1,n} \\ z_{n1} & \dots & \dots & z_{n,n-1} & z_{nn} \end{vmatrix}$$

and the co-factors are obtained by deleting the rows and columns as indicated by the subscripts, and assigning the proper signs. Thus,

$$M_{1n} (= M_{n1}) = (-1)^{1+n} \begin{vmatrix} z_{21} & \dots & z_{2,n-1} \\ \vdots & \ddots & \vdots \\ z_{n-1,1} & \dots & z_{n-1,n-1} \\ z_{n1} & \dots & z_{n,n-1} \end{vmatrix}$$

elements of the matrix which is a consequence of reciprocity:

$$AD - BC = \frac{M_{11}M_{nn} - M_{11nn} D_n}{M_{1n}^2} = 1 \quad (4)$$

Furthermore, if the four-pole is symmetrical or reversible, the driving-point impedance must be the same irrespective of whether the four-pole is excited at the terminals  $1-1$  of mesh 1 or at terminals  $n-n$  of mesh  $n$ . Hence  $D_n/M_{nn} = D_n/M_{11}$ , and therefore  $M_{11} = M_{nn}$  or  $A = D$ .



Fig. 1. General representation of four-pole network.

### 2. Applications of the General Parameter Matrix

The particular types of problems to which the general parameter matrix adapts itself are those involving inter-connection of four-poles in cascade. When four-poles are so connected the input-output relations of the chain are written in terms of the elements of the matrix resulting from multiplication of the general parameter matrices of the individual four-poles in the order of cascading. Assuming for the moment that the 'overall' or 'equivalent' matrix of the entire chain is obtained after such a multiplication, then its elements  $A, B, C, D$  define the following circuit relations, as is obvious from (2);

$A$  is the input-output voltage ratio when output terminals are open;  $A = E_s/E_L | I_L=0$

$$\text{and } M_{11nn} = \begin{vmatrix} z_{22} & \dots & z_{2,n-1} \\ \vdots & \ddots & \vdots \\ z_{n-1,2} & \dots & z_{n-1,n-1} \end{vmatrix}$$

Applying (3) and utilizing elementary determinant algebra one may now obtain a relation among the

MS accepted by the Editor, July 1954

\* This may be regarded as a sequel to the article on "Four-terminal Networks" by O. P. D. Cutteridge in *Wireless Engineer*, March 1953, p. 61.

$B$  is the input voltage required to yield a current of 1 ampere through short-circuited output terminals;  $B = E_s/E_L |_{E_L=0}$   
 $C$  is the transfer admittance;  $C = I_s/E_L |_{I_L=0}$   
 $D$  is the short-circuit current ratio;  $I_s/I_L |_{E_L=0}$

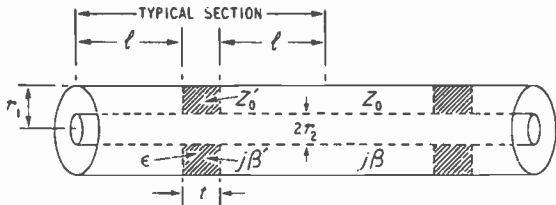


Fig. 2. Coaxial line with dielectric beads supporting the centre conductor;  $Z_0 = 138 \log r_1/r_2 \Omega$ ,  $Z_0' = Z_0/\sqrt{\epsilon}$ ,  $\beta = \omega/3 \times 10^{10} \text{ rad/cm}$ ,  $\beta' = \beta\sqrt{\epsilon}$ .

In dealing with distributed parameter networks, analysis of discontinuity effects is often carried out through use of the general parameter matrix. Consider for instance a loss-less coaxial line employing uniformly spaced dielectric beads, Fig. 2. As a first approximation the effect of the beads can be analysed by replacing each bead by a capacitive susceptance  $j\omega C'$ ,

where  $C' = \frac{\epsilon t}{Z_0 \times 3 \times 10^{10}}$  farads, and  $Z_0$  is the characteristic impedance in ohms of the simple line. This approximation becomes increasingly valid as the electrical length  $\beta't$  of each bead decreases. However, the approximation fails completely as  $\beta't \rightarrow \pi/2$  radians in which instance the bead acts like a quarter-wavelength transformer. A more adequate means of analysing the effect of the beads is to derive the matrix of an entire beaded section which, on the basis of symbols shown in Fig. 2, is done as follows:

$$\begin{bmatrix} A & B \\ C & D \end{bmatrix} = \begin{bmatrix} \cos \beta l & jZ_0 \sin \beta l \\ j \frac{\sin \beta l}{Z_0} & \cos \beta l \end{bmatrix} \begin{bmatrix} \cos \beta' t & jZ_0' \sin \beta' t \\ j \frac{\sin \beta' t}{Z_0'} & \cos \beta' t \end{bmatrix} \dots \quad (5)$$

The actual multiplication of (5) is of no special interest here and will not be carried out. However, it should be noted that the matrix representing the bead may assume forms which imply no interference (it reduces to the unit matrix [1] which has elements equal to unity along the main diagonal, all other elements being zero) or, at the other extreme, impedance inversion (main diagonal elements zero, secondary diagonal elements reciprocals). For this reason approximations should be resorted to only after an examination of prevailing conditions, particularly frequency range.

### 3. Raising a Matrix to a High Power

Let it be required now to derive a general expression for the terminal-to-terminal response

of  $n$  identical beaded sections; a typical section is shown in Fig. 2. The most direct means of accomplishing this is to derive the matrix representing  $n$  identical sections, namely, a matrix representing the original matrix raised to the  $n$ th power:

$$\begin{bmatrix} A' & B' \\ C' & D' \end{bmatrix} = \begin{bmatrix} A & B \\ C & D \end{bmatrix}^n \dots \quad (6)$$

At first sight the operation defined here may appear cumbersome, particularly if  $n$  is large. However, one may apply Sylvester's Theorem<sup>1</sup> and obtain the results required. Let (6) be written more compactly in the form

$$[Q'] = [Q]^n \dots \quad (7)$$

At this point it is pertinent to introduce the characteristic function  $f(\lambda)$  of matrix  $[Q]$ , which is actually the determinant  $f(\lambda) = |Q - \lambda I|$ , and then define the characteristic equation of matrix  $[Q]$  as follows:

$$Q - \lambda I = 0 \dots \quad (8)$$

where the solutions  $\lambda_1, \lambda_2, \dots$  are the latent roots of  $[Q]$  (at times referred to as the characteristic numbers of  $[Q]$ ). In the case under consideration  $[Q]$  is of the second order and hence there will be two latent roots  $\lambda_1$  and  $\lambda_2$ . Returning to (8) and substituting

$$\frac{A - \lambda}{C} = \frac{B}{D - \lambda} = 0 \dots \quad (9)$$

then, in view of (4), one obtains

$$\lambda^2 - (A + D)\lambda + 1 = 0 \dots \quad (10)$$

Sylvester's Theorem provides that

$$[Q'] = [Q]^n = \sum_{r=1}^{r=m} \lambda_r^n [Z_r] \dots \quad (11)$$

where  $n$  is the number of sections interconnected

in cascade,  $m$  is the number of latent roots, and  $[Z_r]$  is a matrix given by

$$[Z_r] = \frac{\prod_{s \neq r} [Q - \lambda_s I]}{\prod_{s \neq r} (\lambda_r - \lambda_s)} \dots \quad (12)$$

Referring to (12) the denominator  $\prod_{s \neq r} (\lambda_r - \lambda_s)$  designates the product of  $m - 1$  factors of the type  $(\lambda_r - \lambda_s)$  with  $s$  assuming all values other than  $r$ . However, in the instance under consideration there are only two latent roots ( $m = 2$ ) so that the denominator of  $[Z_r]$  consists of only one factor. When  $r = 1$  the denominator becomes  $(\lambda_1 - \lambda_2)$  and similarly when  $r = 2$  it becomes  $(\lambda_2 - \lambda_1)$ . The numerator of  $[Z_r]$  in

(12) calls for the product of  $m - 1$  matrices of the form  $[Q - \lambda_s I]$  with  $s$  assuming all values other than  $r$ . Again, since  $m = 2$  the numerator of  $[Z_r]$  consists of one matrix only. Letting  $\lambda_1$  and  $\lambda_2$  be the latent roots of  $[Q]$ , equation (11) is written as follows:

$$[Q'] = [Q]^n = \lambda_1^n [Z_1] + \lambda_2^n [Z_2] + \frac{\lambda_1^n [Q - \lambda_2 I]}{(\lambda_1 - \lambda_2)} + \frac{\lambda_2^n [Q - \lambda_1 I]}{(\lambda_2 - \lambda_1)} \quad (13)$$

It is observed here that  $n$  appears only as an exponent of latent roots  $\lambda_1$  and  $\lambda_2$  and not elsewhere. Furthermore, if the four-pole represented by  $[Q]$  is symmetrical,  $A = D$ , and (10) becomes

$$\lambda^2 - 2A\lambda + 1 = 0 \quad \dots (14)$$

and the two roots are

$$\lambda_1, \lambda_2 = A \pm \sqrt{A^2 - 1} = e^{\pm \gamma}$$

where  $\gamma = \cosh^{-1} A =$  propagation constant of a symmetrical four-pole.

#### 4. Illustrative Examples

A simple and obvious case can be cited here to illustrate the method. Let a loss-less line of

$$[Q'] = [Q]^3 = \begin{bmatrix} -\frac{1}{k^3}(4 \cos^3 \theta - 3k^2 \cos \theta) & -\frac{jZ_0(1 - k^2) \sin \theta}{k^3}(4 \cos^2 \theta - k^2) \\ j \frac{\operatorname{cosec} \theta (\cos^2 \theta - k^2)}{k^3 Z_0 (1 - k^2)} (4 \cos^2 \theta - k^2) & -\frac{1}{k^3}(4 \cos^3 \theta - 3k^2 \cos \theta) \end{bmatrix}$$

electrical length  $\theta$  and impedance  $Z_0$  be represented by a matrix and the latter raised to the  $n$ th power. As in equation (5)

$$[Q] = \begin{bmatrix} \cos \theta & jZ_0 \sin \theta \\ j \frac{\sin \theta}{Z_0} & \cos \theta \end{bmatrix} \quad \dots (15)$$

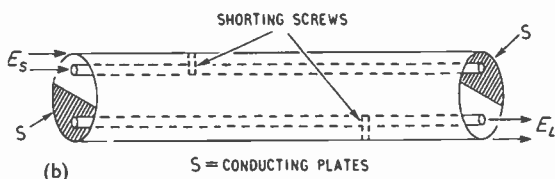
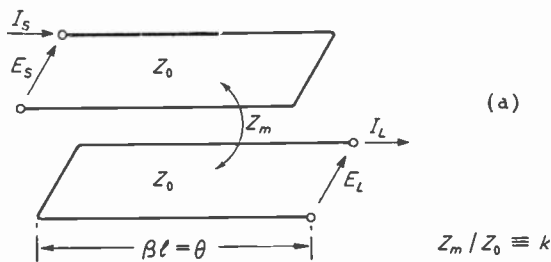


Fig. 3. Coupled-line band-pass filters. Single-section parallel-wire form (a) and three-section screened-pair form (b).

the latent roots are obtained by substituting (15) in (10). They are

$$\lambda_1 = e^{j\theta}; \lambda_2 = e^{-j\theta}$$

Upon substitution in (11) the result is

$$[Q'] = [Q]^n = \begin{bmatrix} \cos n\theta & jZ_0 \sin n\theta \\ j \frac{\sin n\theta}{Z_0} & \cos n\theta \end{bmatrix}$$

as expected. A less obvious case is that related to the coupled-line band-pass filter network of Fig. 3. It has been shown<sup>2</sup> that for this structure

$$[Q] = \begin{bmatrix} -\frac{1}{k} \cos \theta & -jZ_0(1 - k^2) \sin \theta \\ j \frac{\cos \theta (\cos^2 \theta - k^2)}{Z_0(1 - k^2)k} & -\frac{1}{k} \cos \theta \end{bmatrix}$$

and the latent roots become

$$\lambda_1, \lambda_2 = -\frac{1}{k} \cos \theta \pm \sqrt{\frac{\cos^2 \theta}{k^2} - 1}$$

For a 3-section filter, applying (13)

As  $n$  increases the advantage of using this procedure becomes increasingly evident. Another set of expressions for the elements of matrix  $[Q']$ —though not quite as useful—involves hyperbolic and inverse hyperbolic functions, namely:

$$A' = \sqrt{\frac{A}{D}} \cosh (n \cosh^{-1} \sqrt{AD});$$

$$B' = \sqrt{\frac{B}{C}} \sinh (n \cosh^{-1} \sqrt{AD});$$

$$C' = \frac{C}{B} B'; \quad D' = \frac{D}{A} A'.$$

#### 5. Bartlett's Bisection Theorem and the General Parameter Matrix

The usefulness of Bartlett's Bisection Theorem<sup>3</sup> has been demonstrated in many phases of network analysis. At times, of course, bisection in the structural sense cannot be achieved. Thus, in a structural sense, a symmetrical ladder-type structure, or a bridge-T, can be split into two 'halves', whereas a lattice does not allow of this type of bisection, although bisection in the electrical sense is achieved by imposing pertinent electrical conditions<sup>4</sup>. It is of interest to generalize the bisection process by manipulating matrix  $[Q]$  of a four-pole in such a manner as to obtain

the elements of the matrices representing the two 'halves'. This process is completely algebraic and ignores structural aspects. Since the matrices obtained are of the second order, the 'halves' are four-poles, irrespective of the fact that there may be more than two bisection terminals, as in the case of the bridge-T which has three.

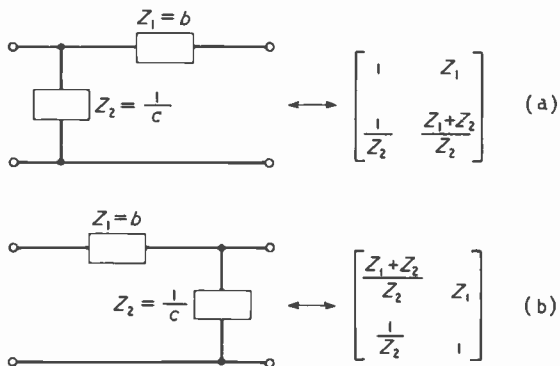


Fig. 4. L-structures and their matrices.

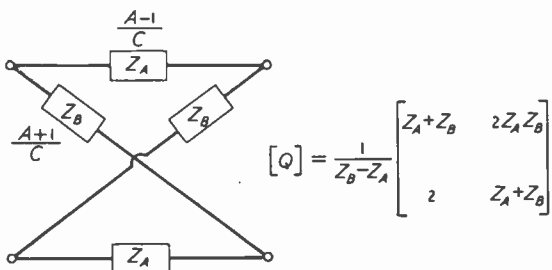


Fig. 5. Lattice network and its matrix.

Let it be assumed that a four-pole defined by matrix  $[Q]$  is bisected. The two 'halves' are defined by matrices  $[Q_1]$  and  $[Q_2]$  such that

$$[Q] = [Q_1] [Q_2] \dots \dots \dots (16)$$

the relation of  $[Q_1]$  to  $[Q_2]$  being that associated with back-to-back connection. Thus if

$$[Q_1] = \begin{bmatrix} a & b \\ c & d \end{bmatrix} \dots \dots \dots (17)$$

it is not difficult to show that

$$[Q_2] = \begin{bmatrix} d & b \\ c & a \end{bmatrix} \dots \dots \dots (18)$$

so that, if,  $A, B, C$  and  $D$  denote the elements of the original matrix  $[Q]$ , (16) requires that the elements of the matrices representing the original structure and the two 'halves' must be related in the manner

$$\begin{aligned} A &= D = 2ad - 1 \\ B &= 2ab \\ C &= 2cd \end{aligned} \dots \dots \dots (19)$$

it being understood that the reciprocity condition  $ad - bc = 1$  restricts the elements of the matrices  $[Q_1]$  and  $[Q_2]$  as implied in (4).

Upon examination of the relations in (19) it is noted that the number of unknown constants exceeds the number of available relations by one. Thus if  $a = 1$  one obtains two 'halves' of the mid-shunt L-type connected back-to-back [Fig. 4(a)], or if  $d = 1$  one obtains two mid-series type L structures [Fig. 4(b)].

Applying (19) to a lattice (Fig. 5) and noting that for the latter the matrix elements are

$$\begin{aligned} A &= \frac{Z_B + Z_A}{Z_B - Z_A} = D; \quad B = \frac{2Z_A Z_B}{Z_B - Z_A} \\ C &= \frac{2}{Z_B - Z_A} \dots \dots \dots (20) \end{aligned}$$

the bisection relations stipulate that if  $a = 1$ :

$$\left. \begin{aligned} b &= \frac{B}{2} = \frac{Z_A Z_B}{Z_B - Z_A} \\ c &= \frac{C}{A + 1} = \frac{1}{Z_B} \\ d &= \frac{Z_B}{Z_B - Z_A} \end{aligned} \right\} \dots \dots (21a)$$

or, if  $d = 1$ :

$$\left. \begin{aligned} a &= \frac{A + 1}{2} = \frac{Z_B}{Z_B - Z_A} \\ b &= \frac{B}{A + 1} = Z_A \\ c &= \frac{C}{2} = \frac{1}{Z_B - Z_A} \end{aligned} \right\} \dots \dots (21b)$$

If now (21a) and (21b) are compared with data shown with Fig. 4(a) and (b) it is obvious that two possible bisection schemes for the lattice are those of Fig. 6(a) and (b).

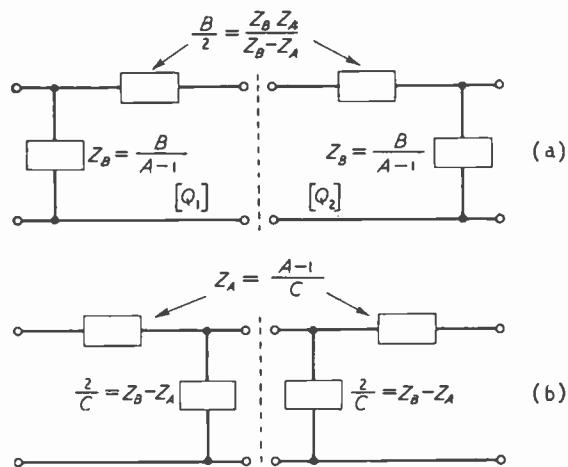


Fig. 6. The two simplest forms of bisected lattice network.

### 6. Back-to-Back Connection

When  $n$  identical but dissymmetrical four-poles are cascaded, impedance matching is achieved by connecting the networks on the image basis, back-to-back. In such a case the matrices of alternate networks are identical whereas the matrices of adjacent networks differ only to the extent that positions of the two elements along

$$\begin{bmatrix} A & B \\ C & D \end{bmatrix} = \begin{bmatrix} \cos \beta_1 l_1 & jZ_{01} \sin \beta_1 l_1 \\ j \frac{\sin \beta_1 l_1}{Z_{01}} & \cos \beta_1 l_1 \end{bmatrix} \begin{bmatrix} \cos \beta_2 l_2 & jZ_{02} \sin \beta_2 l_2 \\ j \frac{\sin \beta_2 l_2}{Z_{02}} & \cos \beta_2 l_2 \end{bmatrix} \dots \quad (28)$$

the main diagonal are interchanged. Referring to Fig. 7, the terminal-to-terminal relations of the entire chain are

$$\begin{aligned} E_s &= AE_L + BI_L \\ I_s &= CE_L + DI_L \end{aligned} \quad \dots \quad (22)$$

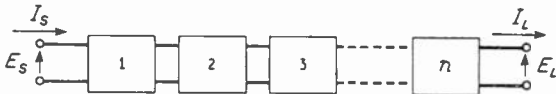


Fig. 7. Cascade of identical dissymmetrical four-poles.

where for the back-to-back connection

$$\begin{bmatrix} A & B \\ C & D \end{bmatrix} = \begin{bmatrix} a & b \\ c & d \end{bmatrix} \begin{bmatrix} d & b \\ c & a \end{bmatrix} \begin{bmatrix} a & b \\ c & d \end{bmatrix} \begin{bmatrix} E_L \\ I_L \end{bmatrix} \quad (23)$$

If the number of sections  $n$  is even ( $n = 2m$ ) the two image impedances of the chain are identical

$$Z_{IS} = Z_{IL} = \sqrt{\frac{ab}{cd}} \quad \dots \quad (24)$$

and (23) becomes

$$\begin{bmatrix} A & B \\ C & D \end{bmatrix} = \begin{bmatrix} a & b \\ c & d \end{bmatrix} \begin{bmatrix} d & b \\ c & a \end{bmatrix}^m = \begin{bmatrix} 1 + 2bc & 2ab \\ 2dc & 1 + 2bc \end{bmatrix}^m \quad (25)$$

whereas if  $n$  is odd ( $n = 2m + 1$ )

$$\begin{bmatrix} A & B \\ C & D \end{bmatrix} = \begin{bmatrix} 1 + 2bc & 2ab \\ 2dc & 1 + 2bc \end{bmatrix}^m \begin{bmatrix} a & b \\ c & d \end{bmatrix} \quad (26)$$

and the image impedances of the chain are distinct

$$Z_{IS} = \sqrt{\frac{ab}{dc}} ; Z_{IL} = \sqrt{\frac{bd}{ac}} \quad \dots \quad (27)$$

### 7. Microwave Structures

In many microwave structures resonance or anti-resonance is achieved through use of short-circuited coaxial line or waveguide sections, although from the theoretical standpoint open-circuited sections serve equally well. Consider a composite coaxial structure such as shown in Fig. 8. Operating as a loss-less cavity in the TEM mode the structure of Fig. 8 will resonate ( $Z_s = 0$ ) provided element  $B$  of the overall

matrix is made zero. This becomes evident by writing

$$E_s = AE_L + BI_L$$

and noting that  $E_L = 0$  (since  $Z_L = 0$ ) and hence for  $E_s = 0$ ,  $B$  must be zero since  $I_L \neq 0$ . Carrying this out, the matrix of the composite structure is written in accordance with notation shown in Fig. 8,

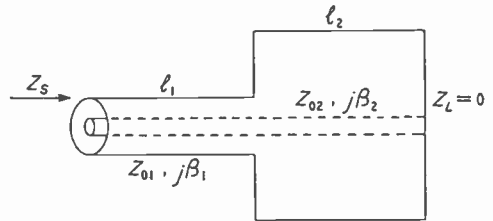


Fig. 8. Composite coaxial structure.

and hence setting  $B = 0$  one obtains

$$Z_{02} \tan \beta_2 l_2 + Z_{01} \tan \beta_1 l_1 = 0 \quad \dots \quad (29)$$

If on the other hand the cavity of Fig. 8 is to become anti-resonant ( $Z_s = \infty$ ), then  $I_s = 0$ , so that relation

$$I_s = CE_L + DI_L \quad \dots \quad (30)$$

stipulates that  $D = 0$ . From (28) this yields

$$-Z_{01} \cot \beta_1 l_1 + Z_{02} \tan \beta_2 l_2 = 0 \quad \dots \quad (31)$$

Cavities closed at both ends are handled in a similar manner. Referring to Fig. 9, the three-section cavity will resonate when element  $B$  of the overall matrix becomes zero. Assuming loss-less sections and noting that  $\beta' = \sqrt{\epsilon} \beta$  and that  $Z_{02} = Z_{01} / \sqrt{\epsilon}$  the resulting relation is

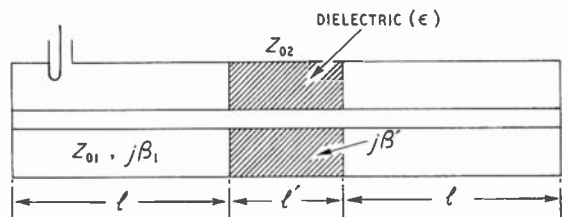


Fig. 9. Three-section cavity.

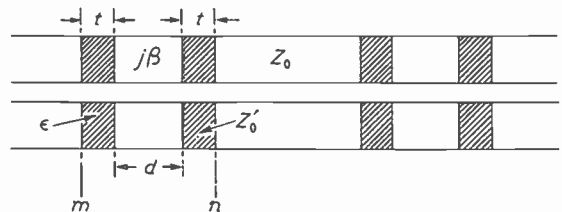


Fig. 10. Beaded line.

$$\cot \sqrt{\epsilon} \beta l' = \frac{1}{2} \left[ \sqrt{\epsilon} \tan \beta l - (1/\sqrt{\epsilon}) \cot \beta l \right] \quad (32)$$

This relation may be utilized to determine permittivity if a variable frequency source is employed.

An additional application of the general parameter matrix deals with impedance matching. Consider the beaded line shown in Fig. 10. The paired beads introduce reflections and if suppression or reduction of the latter is required it is necessary to determine the pertinent relations among variables  $\epsilon$ ,  $l$ ,  $d$  specified in Fig. 10. To achieve this result one obtains the matrix for the line segment  $m-n$ , and denoting the elements of the latter by  $A'$ ,  $B'$ ,  $C'$ ,  $D'$ , one sets

$$\sqrt{\frac{B'}{C'}} = Z_0 \dots \dots \dots (33)$$

where  $Z_0$  is the characteristic impedance of the uniform line. Carrying this out and substituting in (33) symbols shown in Fig. 10 the result is

$$\tan \beta d = \frac{2\sqrt{\epsilon}}{1+\epsilon} \cot \sqrt{\epsilon} \beta l \dots \dots (34)$$

**REFERENCES**

<sup>1</sup> R. A. Frazer, W. J. Duncan, A. R. Collar, "Elementary Matrices", p. 133, The MacMillan Co., New York, 1946.  
<sup>2</sup> J. J. Karakash, "Transmission Lines and Filter Networks", p. 360, The MacMillan Co., New York, 1950.  
<sup>3</sup> A. C. Bartlett, "The Theory of Artificial Lines and Filters", p. 29, John Wiley & Sons, New York, 1930.  
<sup>4</sup> H. Bode, "Network Analysis and Feedback Amplifier Design" p. 266, D. Van Nostrand Co., Inc., New York, 1945.

# CORRESPONDENCE

*Letters to the Editor on technical subjects are always welcome. In publishing such communications the Editors do not necessarily endorse any technical or general statements which they may contain.*

**Differential-Amplifier Design**

SIR,—In his article in the March 1955 issue, Mr. A. M. Andrew comes to the conclusion that there are practical disadvantages which make it difficult to build a differential amplifier that maintains good in-phase rejection without a balancing control. The difficulties appear to be multiplied if operation to z.f. is required.

Possibly it was not known to Mr. Andrew that there already exists a reference in the British literature to a method which avoids many of these difficulties<sup>1</sup>. The basic idea of this work is to feed an in-phase error signal derived from the differential outputs back to the grid of the valve in series with the cathodes of the differential amplifier valves. This inverse feedback of the active-error type<sup>2</sup> tends to reduce the output error proportionate to the gain of the feedback loop. By making this gain sufficiently large, rejection ratios of the order of 10<sup>4</sup> may be obtained over a wide frequency range. Such ratios are almost independent of valve variations, so no balancing control is required. An amplifier making use of two improved versions of this circuit in series has been described<sup>3</sup>. It achieves a composite rejection ratio of the order of 10<sup>8</sup> over a band from 1 c/s to over 100 kc/s and could readily be modified for z.f. operation as well.

J. ROSS MACDONALD

Texas Instruments Inc.,  
 6000 Lemmon Avenue,  
 Dallas 9, Texas, U.S.A.  
 4th May 1955.

<sup>1</sup> E.M.I. Laboratories, "Balanced Output Amplifiers of Highly Stable and Accurate Balance", *Electronic Engineering*, 1946, Vol. 18, p. 189.

<sup>2</sup> J. R. Macdonald, "Active-Error Feedback and its Application to a Specific Driver Circuit", *Proc. Inst. Radio Engrs*, 1955, Vol. 43; to be published.

<sup>3</sup> J. R. Macdonald, "A Multi-loop, Self-Balancing Power Amplifier", *Trans. Inst. Radio Engrs*, Vol. AU-3, *Audio*, 1955; to be published.

**Field-Strength Calculation**

SIR,—I have read with interest the article "Field Strength Calculation" by Kiyohisa Suda in your September 1954 issue. This method necessarily assumes a knowledge of conductivities of ground over mixed paths. While it is true that direct methods have been developed for determining the conductivity of the soil, these methods have certain inherent limitations in their experimental set-ups. Primarily, difficulties have

arisen on account of stray pick-up on the measuring receiver. An accurately calibrated and well-balanced dipole has been tried with some success. The idea of equivalent conductivity put forth by Kiyohisa Suda could perhaps be extended by making measurements in the so-called critical propagation zone for obtaining the conductivities of mixed paths. It would perhaps also be possible by this method to get an idea of stratification of ground in these paths. I believe field strength obtainable is also affected by this factor.

New Delhi,  
 India.

K. L. RAO

15th May 1955.

**Multiloop Feedback Amplifiers**

SIR,—I should like to add a remark in reply to B. D. Rakovich's letter appearing in the May issue concerning Mr. Cutteridge's paper (November 1954) and my letter (February 1955). Referring to the use of the inverse loop amplification function for establishing stability I wrote the characteristic equation in the form

$$A_1 A_2 \left( \frac{1}{Y} - \beta_3 \right) = 0 \dots \dots (1)$$

where

$$Y = \frac{A_1 A_2}{(1 - A_1 \beta_1)(1 - A_2 \beta_2)}$$

It is not proposed to use the entire l.h.s. of this equation as a plotting function, for, as B. D. Rakovich says, this in no way differs from the characteristic function  $1 - A_1 \beta_1 - A_2 \beta_2 + A_1 A_2 \beta_1 \beta_2 - A_1 A_2 \beta_3$  proposed by Mr. Cutteridge. What can be said, however, is that, if  $A_1$ ,  $A_2$ ,  $\beta_3$  are stable minimum-phase functions by themselves, then  $A_1 A_2 \beta_3$  has neither zeros nor poles in the r.h. plane and it follows from (1) therefore that  $1/(Y\beta_3) - 1$  may be taken as the function which must have no zeros in the r.h. plane to ensure stability of the system. The point I wished to make is that  $1/Y\beta_3$  has the advantage of having no poles in the r.h. plane whereas the loop amplification function  $Y\beta_3$  may have poles in that region and the number of these must be previously determined.

I quite agree with the remainder of B. D. Rakovich's letter.

A. J. O. CRUICKSHANK

Department of Electrical Engineering,  
 Queen's College,  
 Dundee.

19th May 1955.

## Transistor Circuit Analysis

SIR,—The following results for the small-signal low-frequency equivalent circuit of a transistor seem to be useful, and so far as the writer is aware, they have not previously been pointed out.

### 1. Input Resistance of an Earthed-Base Amplifier

$$r_i = r_e + (1 - A_i)r_b$$

where  $A_i$  is the current gain of the transistor working into whatever load impedance may be connected. The result is immediately obvious from the equivalent circuit shown in Fig. 1.

### 2. Input Resistance of an Earthed-Emitter Amplifier

$$r_i = r_b + (1 + A_i)r_e$$

This result may be derived in the same way as the previous one.

These formulae are useful because in designing an amplifier it is normally necessary to calculate both  $A_i$  and  $r_i$ , and the standard formulae for  $A_i$  are simpler than those for  $r_i$ . The formulae apply to junction transistors and at least formally to point-contact ones, and are exact, apart from the effects of any approximations made in calculating  $A_i$ . If an external impedance is connected in series with the base or emitter, the formulae still hold if  $r_b$  or  $r_e$  is increased by the value of the impedance, and if the additional impedance is taken into account in calculating  $A_i$ . Shea<sup>1</sup> gives, as an approximation, an expression similar to result (1) but with  $a$  instead of  $A_i$ .

### 3. Earthed-Base or Earthed-Emitter Amplifier Output Resistance

An equivalent circuit is shown in Fig. 2, where  $R_e$ ,  $R_b$  include any impedances, such as source impedances or bias or degenerative impedances connected between emitter or base and earth.

$$i_e = -i_c \cdot \frac{R_b}{R_b + R_e}$$

Hence

$$r_o = (R_e \parallel R_b) + r_c \left[ 1 - a \cdot \frac{R_b}{R_b + R_e} \right]$$

where  $(R_e \parallel R_b)$  denotes the parallel combination of  $R_e$  and  $R_b$ .

This form shows the output impedance as the combination of a passive part  $r_c$  in series with the parallel combination of  $R_e$  and  $R_b$ , and an active part. It also shows that the output impedance is dependent on the ratio of the emitter- and base-circuit impedances, and is essentially the same for earthed-base and earthed-emitter connections.

An alternative form is

$$r_o = (R_e \parallel R_b) \left[ b \frac{r_c}{r_b + 1} \left[ 1 + b \cdot \frac{R_e}{R_e + R_b} \right] \right]$$

where  $b = a/(1 - a)$ .

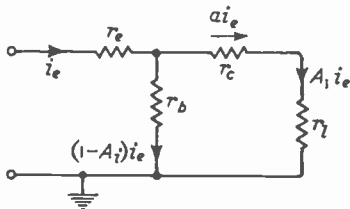


Fig. 1

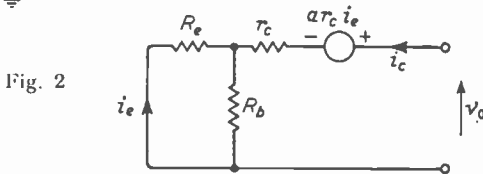
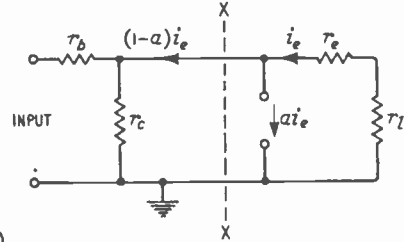


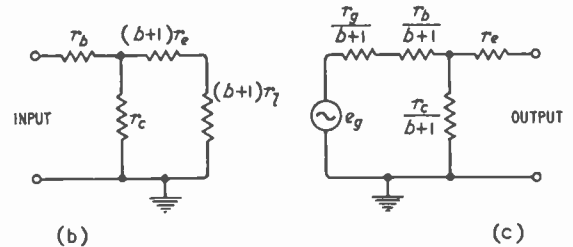
Fig. 2

### 4. Equivalent Circuit of Earthed-Collector Amplifier ("Emitter Follower")

The standard equivalent circuit for a transistor connected as an earthed-collector amplifier working into a load  $r_l$  may be arranged as shown in Fig. 3(a). The portion to the right of the line X-X is equivalent, so far as its effect on the portion to the left of that line is concerned, to an impedance  $(r_e + r_l)/(1 - a)$ , or  $(b + 1)(r_e + r_l)$ . Thus the emitter resistance and the load impedance may be referred to the input side of the transistor by multiplying by  $(b + 1)$ , giving the equivalent circuit shown in Fig. 3(b). The voltage across the



(a)



(b)

(c)

Fig. 3

transformed load impedance in this circuit is equal to the voltage across the actual load impedance in the circuit of Fig. 3(a). Alternatively the generator, base and collector impedances may be referred to the output side of the amplifier by dividing by  $(b + 1)$ , giving the equivalent circuit of Fig. 3(c). These transformations are analogous to the factor  $(\mu + 1)$  which may be used to refer impedances from the cathode to the anode circuit of a thermionic valve.

B. MILLAR

Research Laboratory,  
Associated Electrical Industries Ltd.,  
Aldermaston,  
Berkshire,  
18th May 1955.

<sup>1</sup> Shea, "R.F. Principles of Transistor Circuits," Wiley, 1953.

## The Teaching of Electromagnetism

SIR,—On reading the discussion in the issue of January 1955 by Professor Cullwick and Professor Howe of the question whether the e.m.f. in a 'unipolar' induction experiment is induced in the moving magnet or the stationary external circuit, it seemed to us simpler to discuss pure translation. This often yields straightforward useful results, as in the case treated by Professor Cullwick in his book "The Fundamentals of Electromagnetism" (Cambridge 1949) and taken further both by ourselves and by him to illustrate the secondary nature of the concept of the magnetic field. (*Brit. J. Appl. Physics*, Vol. 2, p. 330, 1951.)

Consider a long bar magnet which moves at right angles to its axis. To a stationary observer, it acquires a relativistic electric moment normal both to its axis and

# NEW BOOKS

its direction of motion. It should be possible, one would think, to produce from such an electric dipole a current in a stationary circuit by means of two sliding contacts. A current does indeed appear if the stationary circuit passes in front of a pole-face but is absent if the circuit is confined to a region remote from the pole-faces. Expositors of the 'bristle' theory and of induction in circuit elements naturally take this case to support their views. Equally, on the other hand, it can be stated that a stationary observer in front of the pole-face perceives an electric field but the stationary observer remote from the pole-face does not. This shows that although the electric dipole is associated with the magnet the interpretation of the concept needs care. The advantage of the magnetic field concept, though secondary, is that it enables one to deal with a complete circuit in usually, but not always, a fairly simple way without studying what different observers may perceive and, thence, to deduce what electrons or other charged particles may experience in their vicinity.

The rotating magnet introduces a more complicated kind of motion. Sometimes rotation can be studied by applying principles appertaining to translation, but not always. R. Oppenheimer has given an example (inadequately\* discussed by Schiff, *Proc. Nat. Acad. Washington*, Vol. 25, p. 391, 1939) of two concentric hollow spheres with equal and opposite surface charges uniformly distributed and bound to the surfaces. If they rotate about a diameter, a stationary observer perceives a magnetic field outside the outer sphere. On the other hand if the spheres are at rest and the observer and his system rotate about a diameter of the spheres, he will perceive no electromagnetic field outside the spheres. The relative motion is here not interchangeable as it would have been for pure translation.

Although probably most problems of engineering interest can be dealt with by principles appertaining to translatory motion, including the classical rotating disc and rotating magnet of Faraday, yet there is a danger. The difficulty is that a book dealing rationally with the elements of the relativistic principles of electromagnetism in rotation has yet to be written. Naturally the equations of general relativity applied to electrodynamics comprise all the basic theory. A curious result of these equations in a rotating system is an additional force on a moving charge, proportional and parallel to its velocity (rather analogous to a positive or negative resistance) which is usually extremely small†.

Indeed one is led rather to the view, which Professor Howe seems to share, that it would be extremely confusing to students, not specializing in relativity theory, to encourage them to learn and use anything beyond the one or two simple examples which clearly and easily illustrate the unification of electromagnetic concepts which relativity can provide.

H. PELZER  
S. WHITEHEAD

The Electrical Research Association,  
Greenford,  
Middlesex.  
16th May 1955.

\* Schiff obtains the obviously wrong result that the rotating observer (in the second case) would find the field to vanish at any point. But obviously he must find a non-vanishing field in the space between the two spheres. Schiff mentions but fails to use the mixed tensor mentioned in the next footnote and so artificially retains the form of Maxwell's equations, but in co-ordinates which do not exist.

† This novel component is possible because in the equation for electromagnetic force [e.g., Tolman, "Relativity Thermodynamics and Cosmology", p. 260, equ. (103.1) or Eddington, "Mathematical Theory of Relativity", p. 190, equ. (80.1)] occurs the mixed tensor  $F_i^k$  instead of the covariant tensor  $F_{ik}$  or the contravariant tensor  $F^{ik}$ . The mixed tensor is no longer antisymmetric and the diagonal elements do not necessarily vanish in a rotating system, whence the force mentioned is not necessarily zero as is the case in classical electromagnetic theory or in the relativistic theory of translational systems.

## Schaltungstheorie und Messtechnik des Dezimeter- und Zentimeterwellengebietes

By Dr. ALBERT WEISSFLOCH. Pp. 308 with 288 illustrations. Verlag Birkhäuser, Basel, Switzerland. Price 33.50 Swiss francs.

This is one of a series of textbooks and monographs on the exact sciences. Although the author is German by birth and education and has been with Siemens Schuckert and Telefunken, he has been in France since 1947, and is technical director of a French company engaged in electronic research and applications. The book is divided into four chapters, of which the first of about 80 pages deals very fully with the theory of four-pole networks, based mainly on linear fractional functions and the geometry of the circle. The second chapter deals with the theory and measurement of uniform transmission lines of various types, with special reference to waveguides; here also geometrical methods are employed based on circular, elliptical, hyperbolic and parabolic sets of curves. The effects of various types of discontinuities due to changes of cross-section, bends, insertion of conducting or dielectric elements, are fully discussed.

The third chapter deals with the series connection of four-poles and discusses the transformation properties of the insertion of dielectric discs and metallic objects in waveguides. Six- and eight-pole networks are then discussed, the magic tee, Bethe hole coupler, the linking of circular and rectangular waveguides, hollow resonators, and high-frequency filters. The final chapter deals with matching and we must point out that near the beginning of the book on page 12 there is a printer's error; it says that for maximum output  $R_r = R_i$  where  $R_r$  is the impedance of the load at the generator terminals and  $R_i$  is the internal impedance of the generator; this should be  $R_r = \bar{R}_i$  where  $\bar{R}_i$  is the conjugate of  $R_i$ . After dealing with matching the author discusses the application of resonance to measurements, the self-excited oscillator and its frequency stability, and waveguide transforming and coupling with special reference to broad-band operation.

An interesting detail is that  $I_1$  and  $V_1$  always refer to the output and  $I_2$  and  $V_2$  to the input to the line; the author says that he adopts this order because the treatment of the problem nearly always begins at the output and works back to the input.

A large number of references are given as footnotes throughout the book.

This is certainly a book that can be recommended to anyone with the necessary knowledge of German.

G. W. O. H.

## Wireless and Electrical Trader Year Book 1955

25th Edition. Pp. 304. Trader Publishing Co. Ltd., Dorset House, Stamford Street, London, S.E.1. Price 12s. 6d.

## Metal Industry Handbook and Directory 1955

Pp. 472. Published for *Metal Industry* by the Louis Cassier Co. Ltd., Dorset House, Stamford Street, London, S.E.1. Price 15s.

## National Bureau of Standards Biennial Report 1953 and 1954

Pp. 162. National Bureau of Standards Miscellaneous Publication 213. Superintendent of Documents, U.S. Government Printing Office, Washington 25, D.C., U.S.A. Price 60 cents.

## BRITISH STANDARDS

**Electric Signs and High-Voltage Luminous Discharge-Tube Installations**

B.S. 559:1955. Price 5s.

**Electronic Valve Bases, Caps and Holders, Sections B3G and 4.**

B.S. 448:1955. Price 1s.

**Glossary of Acoustical Terms**

B.S.661: 1955. Price 6s.

**International Electrotechnical Vocabulary**

2nd Edition. No. 50(12) Transducers. Price 7s. 6d.

Obtainable from British Standards Institution, 2 Park Street, London, W.1.

## "MATERIALS HANDLING NEWS"

The first issue of a new quarterly journal *Materials Handling News* is published on 1st July by *Mechanical Handling*, Dorset House, Stamford Street, London, S.E.1. It has a newspaper format and the first issue deals with such matters as the reduction of handling costs, organizing the loading and unloading of lorries, and the gain of mechanization.

## BIRTHDAY HONOURS

In the Birthday Honours List, a baronetcy is conferred upon Sir George Nelson (Head of the English Electric-Marconi group of companies).

Harold Bishop (Director of the B.B.C. Technical Services) is appointed a Knight Bachelor.

Hugh K. Grey (Head of the communications department, Foreign Office), F. N. Sutherland (General Manager, Marconi's Wireless Telegraph Company) and J. N. Toothill (General Manager, Ferranti, Ltd.) are appointed Commanders of the British Empire.

Philip H. Spagnoletti (Director and General Manager, Kolster-Brandes) becomes an Officer of the Order of the British Empire. Harold W. Cox (E.M.I. Engineering Development), Richard W. Lewis (Chief Chemist, Burndept) and Robert J. Parker (Senior telecommunication superintendent, Cable and Wireless (G.P.O.), Birmingham) become Members of the Order of the British Empire.

## APPOINTMENTS AND AWARDS

Dr. A. L. Cullen has been appointed to the chair of electrical engineering in the University of Sheffield.

Rudolph Kompfner has been awarded the Duddell Medal by the Physical Society in recognition of his work in this country on the travelling-wave valve. He first described this in *Wireless World* for November 1946 and, in more detail, in *Wireless Engineer*, September 1947.

The Senate of the University of London has conferred the degree of D.Sc. (Engineering) on Dr. A. Rosen, Consultant Engineer (Telecommunications) British Insulated Callender's Cables Ltd., for his work in the field of telecommunication cables.

## BACK TO NORMAL

This copy of *Wireless Engineer* should appear in the normal way and at the normal time. Last month's issue may have reached some readers late because of distribution difficulties, for which it is hoped they will blame neither publisher nor newsagent.

## INSTITUTE OF PHYSICS

Sir John Cockcroft (Director of the Atomic Energy Research Establishment) has been re-elected President of the Institute of Physics for the second year in succession. Dr. W. H. Taylor has been elected a vice-President; Dr. S. Whitehead and Dr. B. P. Dudding have been re-elected Honorary Treasurer and Honorary Secretary respectively.

## INSTITUTION OF ELECTRONICS EXHIBITION

The tenth annual Electronics Exhibition will be held at the College of Technology, Manchester, from 14th to 20th July, except 17th July, from 10 a.m. to 10 p.m. on most days. On 16th July the exhibition will close at 6 p.m. and on 14th July it will open at 2 p.m.

There will be two sections to the exhibition—scientific and industrial research and manufacturers. Tickets are obtainable from W. Birtwistle, 78 Shaw Road, Thornham, Rochdale, Lancs.

## STANDARD-FREQUENCY TRANSMISSIONS

(Communication from the National Physical Laboratory)

Values for May 1955

Date 1955 May	Frequency deviation from nominal: parts in 10 <sup>8</sup>		Lead of MSF impulses on GBR 1000 G.M.T. time signal in milliseconds
	MSF 60 kc/s 1429-1530 G.M.T.	Droitwich 200 kc/s 1030 G.M.T.	
1	+0.1	+3	NM
2	+0.1	+4	+25.8
3	+0.1	+4	+26.4
4	+0.1	+3	+27.9
5	+0.1	+4	+28.1
6	+0.1	+3	+28.2
7	+0.1	+3	NM
8	+0.1	+4	NM
9	0.0	+4	+29.7
10	0.0	+4	+29.3
11	0.0	+4	+31.2
12	+0.1	+4	+31.9
13	+0.1	+5	+32.2
14	NM	+5	NM
15	+0.1	+5	NM
16	NM	+5	NM
17	NM	+5	NM
18	0.0	+5	+32.9
19	0.0	+1	+33.2
20	0.0	+1	+34.4
21	0.0	+1	NM
22	0.0	+1	NM
23	0.0	+1	+35.8
24	0.0	0	+36.3
25	+0.1	+1	+37.3
26	+0.2	+1	+37.1
27	NM	+1	NM
28	+0.2	+1	NM
29	+0.2	+1	NM
30	+0.2	+1	NM
31	+0.2	0	+40.9

The values are based on astronomical data available on 1st June 1955.

NM=Not Measured.